Doctoral Dissertation

Development of aromatic biopolybenzazoles showing ultrahigh thermoresistance and dielectric performance

ZHONG Xianzhu

Supervisor: Tatsuo Kaneko

Japan Advanced Institute of Science and Technology

Graduate School of Advanced Science and Technology

Material Science

June 2022

ABSTRACT

Bio-materials are of great significance for sustainable development of society due to the restriction of fossil fuel-based resources. Tremendous efforts have been focusing on developing bio-based materials have comparable performance with fossil fuel-based materials. Work in this thesis described the syntheses and characterizations of bio-based polybenzazoles with high thermal resistance and dielectric performance.

In chapter 2, conventional 2,5-polybenzoxazole and new 2,6-polybenzoxazole were synthesized from bioderived 3-animino-4-hydroxylbenzoic acid and 4-amino-3-hydroxylbenzoic acid respectively. There is no significant difference between there thermal resistance in homopolymer state. However, after copolymerized with polybenzimidazole, in the same molar composition, 2,6-polybenzoxazole-*co*-polybenzimidazole presents an obvious higher thermal decomposition temperature than 2,5-polybenzoxazole-*co*-polybenzimidazole, the highest 10% mass loss temperature reaches 740 ℃, the obtained copolymer can be used to fabricate pliable film, suggesting this copolymer is promising to be utilized as thermoresistant materials.

In chapter 3, polybenzothiazole was synthesized from bio-based resources for the first time. The precursor monomer 4-amino-3-mercaptobenzoic acid was synthesized from bio-derived 4-aminobenzoic acid, and the obtained monomer was copolymerized with PBI and obtained a series of copolymers. The thermoresistance and dielectric properties were characterized. The copolymer presents an increasing thermal stability as increasing the amount of PBI, this is probably due to existence of hydrogen bond elevated the thermal stability. Besides, polybenzothialzole-co-polybenzimidazole presents dielectric around 3, lower than most of the dielectric polymers. This is probably due to the low-polar structure of thiazoles, enhanced the dielectric performance of the copolymers.

In chapter 4, terpolymer poly{benzimidazole-*b*-(benzoxazole-*r*-amide)} with a block structure was synthesized with a stepwise terpolymerization of 3 monomers. The obtained terpolymers present ultrahigh thermal resistance, and the thermoresistance increases with the increasing molar compositions of polyamide, the mechanism of this was revealed by DFT calculation, the result indicate that the appropriate amount incorporation of polyamide can impede the resonance effect and thus increase the molecular interaction enthalpy, as a result, the thermal stability is enhanced, the high thermoresistance is attributed to the hydrogen bonds. Besides, the dielectric constant of the terpolymers vary within 2.4 to 3, showing an outstanding dielectric performance. Considering the high performance in both thermal and dielectric properties, the terpolymer was successfully utilized as a coating material for copper coil, indicating the terpolymer is promising to be used as thermostable insulating materials.

Keywords: polybenzazoles, thermoresistance, low-*k*, copolymer, terpolymer, H bond

CONTENTS

Chapter I

General introduction

Chapter I

1.1 Plastic

Plastics are perfect substitutes for metals, glasses and wood products. As a series of synthetic or semi-synthetic materials, plastics always have polymers as the main ingredient, making it possible for them to be processed complicatedly and intricately to meet the increasing demands for industry. Plastics are well known due to the unique properties, for instance, adaptability, they can be easily compressed, extruded or moulded into objects of any shapes; lightweight, plastics are much lighter than other materials in the same volume; durability, plastics are more capable of enduring rough operation compared with woods; flexibility, plastics are elastic and easy to proceed; low-cost, they are inexpensive to produce.[1–5] These properties have led widespread use all over the world.

Generally, plastics are produced by human industrial system from the precursor material derived from fossil fuel-based chemicals--petroleum and gas. The crude resources such as oil is proceeded to obtain the precursor monomers such as ethylene and propylene, and these monomers can be polymerized to obtain polyethylene (PE) and polypropylene (PP), which are representative plastics widely used in various applications. However, during the production, many raw materials are converted in vain to thermal energy and

carbon dioxide, which leads to a great waste and greenhouse effect. Besides the low energy efficiency, the sustainability is threatened due to the depletion of fossil fuel, the petroleum is consuming at a speed of approximately 36 million barrels per year and will run out in 40 years.[6–9]

For the sustainable development and high effectively use of petroleum source, it is of great significance to develop plastic materials that are eco-friendly and can be obtained from recycled sources.

1.2 Bioplastics

As is discussed above, fossil fuel-based plastics are no longer available due to resources depletion, which has become an urgent problem to be settled, attracting increasing concern over global. In order to achieve the sustainable development, it is necessary to build a recycling society that can take full advantages of the unlimited natural resources. Bio-plastics are plastic materials that obtained from natural renewable biomass resources, such as botanical sawdust, straw, maize starch, vegetable fat and oil food waste, and bacterial derivatives, have been considered to be a promising candidate for replacing the fossil-fuel plastics (petro-based plastics). [10]

Bioplastics can be obtained from natural resources through many ways. Some of them are obtained via the direct processing of naturally produced bio-polymers, mainly

including 2 types: polysaccharides, such as alginate, chitosan, starch and starch; proteins, such as gelatin, gluten protein etc. bioplastics can also be obtained via chemical synthesis from sugar and the derivatives such as lipids (animal and vegetable oils, fats), lactic acid and etc. [11–14]

The largest advantage of bioplastics is their sustainability. The resources for producing bioplastic will never deplete as long as the plants and bacteria are photosynthesizing and storing energy (**Figure 1.1**). Besides, some bio-based plastics are degradable and recyclable, which is distinct properties that conventional petroleum-based plastics don't possess. With the depletion of petroleum, renewable bioplastics play a more and more important role in the future. [15]

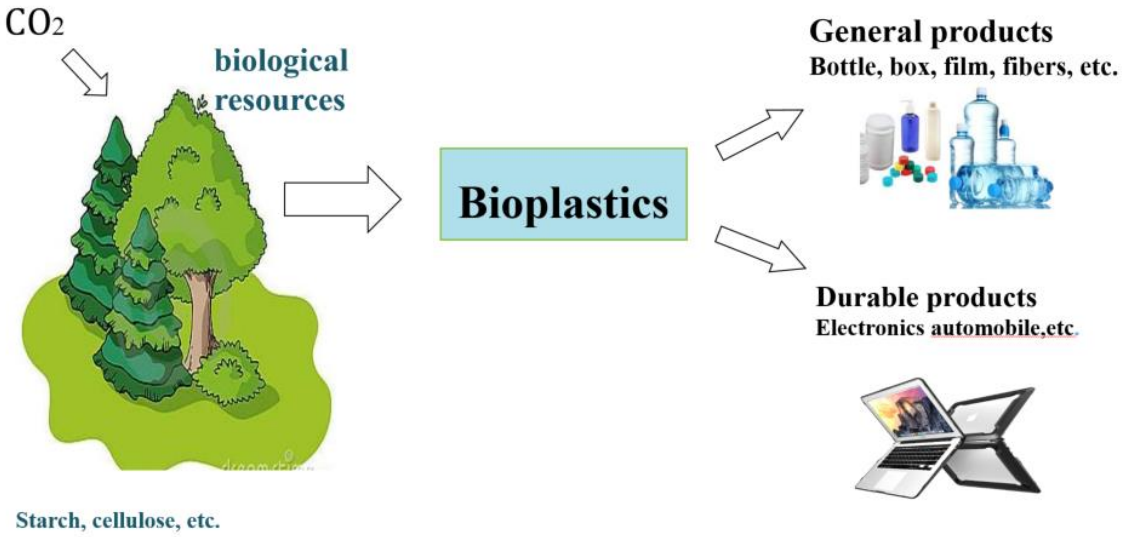

Figure 1.1. Bioplastics obtained from nature.

1.2.1 Polysaccharides-based bioplastics

The most representative bioplastic is thermoplastic starch, which is widely applied and account for 50% in the market.[16,17] The preparation of this material is simple, it can be obtained via gelatinizing starch and further solution casting, which are feasible chemical experiments that can be operated at simple condition. Pure starch is strongly humidity absorbing and therefore a good candidate as the material for producing drug capsules in the pharmaceutical industry. However, pure starch polymer is restrained in applications for its high brittleness and thus plasticizer (e.g. glycol, sorbitol) is added so that starch based bioplastics can be processed to satisfy, the resulting starch-based bio polymer materials is able to be tailored for the specific purpose through adjusting the type and amount of the addictive plasticizers. Besides, due to the high operability, processing techniques (e.g. extraction, injection molding, solution casting, compression molding) for petro-based plastics is also available for starch biopolymer materials. The

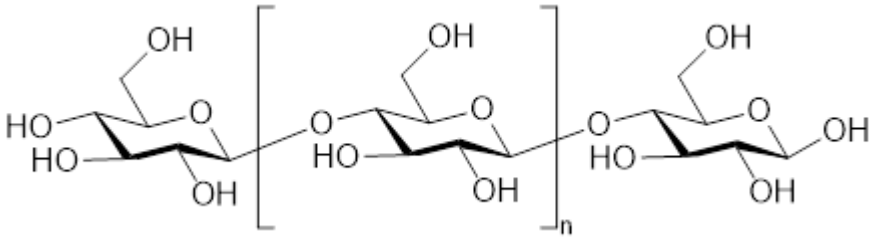

Figure 1.2. Molecular structure of polysaccharide

characteristic of the obtained material is highly impacted by the amylopectin/ amylose compositions, high amylopectin ratio results a stronger mechanical flexibility and operability while high amylose ratio leads a polymer with lower processibility (**Figure 1.2**).

Starch-based polymers composite are usually made through blending with some decomposable polymers. The composites such as Ecoflex/starch, polylactic acid/starch are widely applied for industrial purpose, for example, starch bioplastics are widely used for packaging, they are not only endurable in use and also highly degradable and ecofriendly for the environment.[16–20]

Besides starch-bioplastics, cellulose-based plastics are also an important number of polysaccharides-bioplastics. Cellulose acetate, nitrocellulose, and their derivatives constitute the cellulose bioplastics. In spite of the excellent mechanical properties, cellulose is rarely solely used for packaging due to the high price, instead, they often work as addictive for other material such as starch to form a blend with improved mechanical performance, the resulting blend can be a good candidate for packaging material due to the mechanical properties and low price.[21–25]

Other polysaccharides (e.g. chitosan, alginate) based plastics are also well investigated for industrial usages.[26] Chitosan can be processed into designed shape by the

conventional techniques due to the high processibility, especially film form, chitosan exhibits a high film forming ability in solution casting. Researches indicate that the addition of chitosan to other plastics can increases the service life of plastics. Considering it is the second most abundant polysaccharides on earth, chitosan is perfect alternative for packaging material. Alginate shows the alike properties and can be processed into plastic form, when blending with restrained amounts of plasticizers or water, alginate is highly processible. [27–29]

1.2.2 Protein-based plastics

Protein-based plastics is considered to be available in the future (**Figure 1.3**). Raw material can be easily obtained for nature, for example the casein and gluten of wheat exhibit excellent properties for making biopolymers. Besides, soy protein is also investigated as the source for making bioplastics.[30–32] This kind of protein has a long

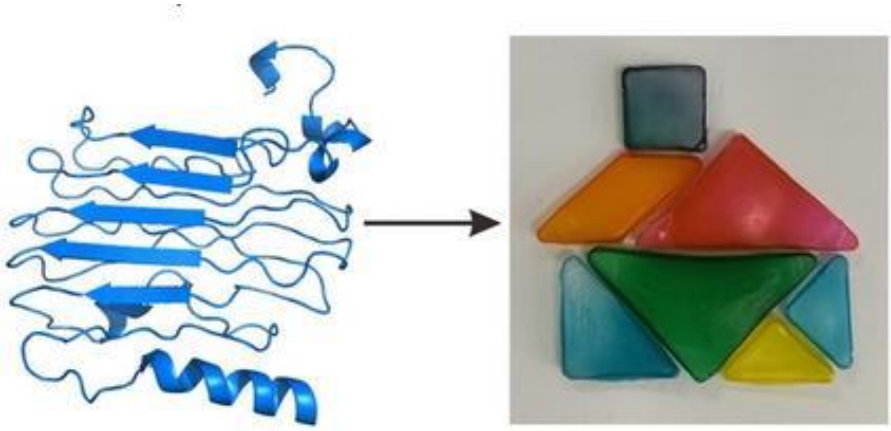

Figure 1.3. Proteins is one of the resources of bio plastics.

history to be utilized in plastic production, for instance, Ford industry made a body-panels from soy protein-based bioplastics for automobiles. However, protein-based plastics are restrained in use up to now due to the strong water sensitivity and high cost.

1.2.3 Aliphatic bioplastics

Aliphatic bioplastics is the aliphatic polymer materials possesses a aliphatic backbone. Generally, aliphatic bioplastics are aliphatic polyesters, mainly including polylactic acid (PLA), polyhydroxyvalerate (PHV), poly-3-hydroxybutyrate (PHB), polyamide (PA) etc. PLA is a kind of transparent bioplastic derived from corn or glucose, it is alike to conventional fossil fuel-based plastics such as PS. PLA is sustainable and biodegradable but inferior to the conventional plastics in impact strength. PHB is a polyester that produced when processing maize starch, glucose or wastewater with bacteria. It has analogous properties with some other polyhydroxyalkanoates and distinguishes primarily by its physical properties that melting point of PHB comes higher than 130 degrees Celsius. Polyamide 11 is a kind of biopolymer derived from natural oil. PA11 is different from the regular bioplastics, it is an important member of the nylon family, formed through the polycondensation of 11-aminoundecanoic acid, which is obtained from castor beans. Due to the outstanding thermo-mechanical performance (melting point: 180-190 °C, elongation at break: 300-400%), PA 11 is widely utilized in varies of

fields such as electrical, coatings, aerospace transportation etc. [25,33–36]

In spite of the small amounts of usages in the market compared with the fossil fuel plastic, the researches on bioplastics continues. Bioplastics constitute less than 1% of the entire plastics manufactured and applied worldwide due to the high cost and relatively low thermo-mechanical properties compared with the conventional fossil fuel-based plastics. Giving the sustainability of material, it is of great significance to explore the bioplastic with high thermo-mechanical performance. [37–40]

1.3 High thermoresistant polymers

High thermoresistant plastics are a specialized and rapidly growing segment of the plastics market. Thermoresistant polymers have been widely used in various of fields, among all the application, the aerospace presents the main impetus for the research and development of this type of material. Preparations and explorations of high thermoresistant polymer have been lasting for decades, but difficulties have been encountered in the process, such as the insolubility of thermoresistant polymers, relatively constrained market and high cost for the products. The progress has been heavily limited by the imperative requirements, the solubility and processibility. [13,25,40,41]

Generally, polymers with high thermal stability tend to convey a chemical structure that is not soluble or fusible, and therefore the modifications on the structure are performed

to achieve the fabrication.[42] As a result, only few of the polymers have been fully investigated and commercially available. To our best knowledge, in the past decades, there is little novel high thermal resistant polymers have been synthesized or developed with completely new structure. most of the works concentrate on the improvements or modifications on polymers with known structures, making them easier to be processed and fabricated with less loss on the thermal stability. However, in spite the efforts, the thermal stability of polymers is not significantly enhanced through the present measures.[40,43–46] Giving the difficulties in development of high thermal resistant polymer materials, the polymers with high thermal resistance must meet the following requirements: the first is the retention of mechanical performance, high softening temperature and high glass transition temperature. The second is the high resistance to thermal degradation, and the third is the high resistance when exposed to chemical attack, such as oxidation, hydrolysis.

Table 1.1. Bond energies of various chemical bonds (KJ/mol).

C-S	273	C-N	307	C-H	416	P-O	528	C=C	609
B-H	294	Si-H	319	C-F	428	P-C	580	C=N	617
		Si-C	328	Si-N	437			Ti-O	672
		C-C	340	Si-O	445			B-O	777
		C-O	361						
		C-B	374						
		B-N	386						

Generally, glass transition temperature (T_g) is domaining the maximum heat resistance of polymer material in most practical usage. T_g is able to be improved by enhance inter molecular forces between chains.[47–49] The most known approach is to incorporating extra polar side groups into the molecular backbone. For example, the glass transition temperature of atactic polypropylene is approximately -20 degree Celsius, however, after introduction of -CN, the glass transition of polyacrylonitrile increases to about 105 degrees. H-bond is increased the chances to happen by chemical crossing-linking of the inter polymer chains.[50] Other approaches are mainly to optimize the regularity of polymer chains and thus increases the crystallinity, in this case, the thermal resistance can be elevated but the polymer chain become more rigid. [51–53]

Chemical bond strength is greatly influencing the thermal resistance. To obtained a higher thermal stability, the constitution of bonds with weak strength should be avoided or reduced to the minimum amount. **Table 1.1** shows the chemical bond strength of the most common bonds, if solely emphasis the bond strength, it tends to occur the concentration of developing inorganic materials instead of organic polymer materials. In essence, the stronger is the bond, the more likely not offset by chemical attack in the process of relatively low activation energy reactions, such as oxidative cleavage or hydrolytic reactions. Siloxanes are the most known compound with a complete

inorganic backbone present the example of the dangers of concentrating on bond energy and excluding the other factors. In polysiloxane the Si-O bond energy is 445 kJ/mol and that of the Si-C is 328 KJ/mol, Si-C would therefore be expected to cleave more preferentially than Si-O and eliminate the alkyl. However, in practice, Si-O bond cleaves more preferentially and results in the formation of cycle product with low molecular weight, this is because this is the reaction that more energetically supported[50,54,55].

The properties of the model compounds give the other pointers to thermostable structures. The drawback is that, from the behavior of the compounds, it is hard to predict the effects brought by the degradation happened in the polymer chains. In a strict chemical sense, a complete chemical compound is extremely difficult to be prepared as polymer. Apart from the problems of molecular weight and its distribution, the polymer chain is possibly end up with different functional groups, special configurations, branching structure, the existence of impurities resulted from initiator chemicals, side products etc. [45,56]

Therefore, to obtain a compound with high thermal stability, the following factors can be taken into account in the perspectives of chemistry:

i The strong bonds should be used as much as possible.

ii The easy paths for the rearrangement reactions should be avoided.

iii Resonance should be adapted in the structure to the maximum.

iv All the rings in the structure should be arranged in normal angles.

v Molecular weight should be as higher as possible.

Among all the conditions, (i) is seldom the dominating one. Most chemical bonds have enough strength to give sufficient stability provided that the only possible decomposition mechanism involved bond break as the first step, and that this step is not followed by the small simple fragments elimination, which is a chain reaction.[52] Almost all the configuration systems break down owing to operative less energetic mechanism, refers to condition (ii). Resonance stabilization (iii) is always positive because it leads to larger consumption of energy at bond capture and if bond angles are normal (iv), then once the natural structure angles which fixes the atoms in close proximity is broken, it is possible that the bond healing would occur as long as the excess energy was dissipated in the molecular.[53,57,58] In polymer configuration, skeletal atoms are required to link in the chain by multiple routes to ensure that the chain will not be cleaved in a capture of one single angle bond. It must be emphasized that all these conditions mentioned really involved in a perfect structural unit in isolation. In fact, a ideal structure seldom does a polymer attain due to the interactions between or within molecules. Nevertheless, the

data is clear enough for the conclusions drawn relating polymer structure with its thermal resistance. [59–62]

Chains consist of para-linked rings tend to present the highest thermoreisitance, such structures also bring the highest softening points, the lowest solubility, as well. To appropriately compromise the stability and fabrication, meta-structured units are often introduced to replace a part or all of the para linked-rings. Rings with hydrogen substituents often give the optimum thermal resistance. Substitution of hydrogen by any other function group or atom usually results in reduction in polymer thermal stability. Hydrogen substituent often become more active at elevated temperatures in oxidizing atmospheres.[61] In thermostability criteria, the weight loss results obtained are to a degree impacted by experimental parameters and also by polymer features listed as follows:

i. Molecular weight. The effect of degradation depends on whether initiation of breaking down is preferentially occurred at chain ends, or at the point of defect and irregularity. It also depends on whether initiations are followed by the depolymerization of the polymer chains.
ii. Chain branching. An appropriate amount of branches bring little effect, but stability decrease as the number increases to a certain degree.

iii. Cross-linking. Just as branching, some amount of crosslinking bring a slight influence, but decrease as the amount increases

iv. Crystallinity. The degree of crystallinity has a great impact on the thermo-oxidative stability.

v. Trace impurities. Impurities can be very deleterious for the stability, they always bring with reduction in stability due to various reasons.

vi. Structural changes as the degradation proceeds. This can be accounted for changes observed in the apparent whole activation energy for breaking down during the process of a reaction.

Generally, aromatic polymers tend to exhibit higher thermal resistance, which is usually gained from the introduction of aromatic chains instead of aliphatic chains in their molecular backbone (**Figure 1.4**). This change restrained the mobility of the molecular chain and on the meanwhile, 2 chemical links are required to be broken for a complete

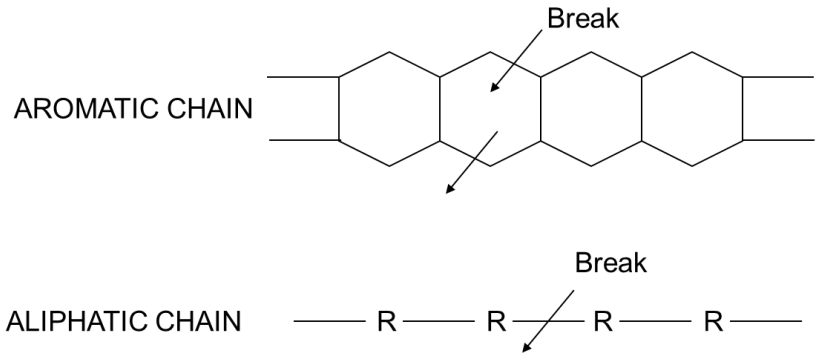

Figure 1.4. Illustration of bond breaking.

chain break, as a result, more energy is demanded, and the aromatic chain can endure a

higher temperature compared with the aliphatic chain.[41,63–66]

1.4 Low-*k* material

Low-*k* material is the material having small relative dielectric constant, which is usually used as an index for dielectric performance of materials.[67] The application of low-k material is one of important strategies for the continued scaling of microelectronic devices, colloquially referred to the extension of Moore's law. In electronic digital circuit boards, conducting parts is separated from another by insulating dielectric materials, to avoid the short circuit which possibly cause severe damage to the digital circuit. [68–71] The development of microstructure chip request a densely stacked electric component, where an adverse influence to the performance of devices may advent due to the crosstalk or charge build up as the dielectrics thinning to a degree. Instead of conventional silicon dioxide, a low-k polymer material with the same size requests a lower parasitic capacitance, which brings faster speed in switching and lower heat dissipation.[72]

Tremendous efforts have been made in the development of polymer low-k dielectrics from 1990s. In spite of the wide use of inorganic silicon dielectrics, organic low-k materials show significant advantages, such as low-cost, higher solution processability,

easy to process and fabrication, and possible modification on the polymer chemical structure to attain the requested material properties. Previously, several polymeric materials, such as SILK (k = 2.65, Dow Chemical), polyimide (PI), polybenzobisoxazole and polysilsesquioxane have been developed as low-k dielectric materials. However, the k value needs to be further reduced for the wide range applications, many works have been done on the reduction of the k values. The most common approach to reduce the k value is to introduce the nanosized air voids (with a k value of approximately 1.0) into the low-k polymer materials.[73,74] The k value of such porous polymer materials can be less than 1.5. (25−31) However, the introduction of nanosized air voids is too complicated to perform, it is difficult to control, and expensive. Furthermore, these operation results adverse impact on the polymer materials, the size, structure and nanopores distribution would greatly affect the texture homogeneity and thermal stability of low-k polymer materials.[75] Besides, in this method, too much nanosized pores in the bulk will also case a damage in polymer mechanical properties and promote the moisture absorption, which often result in deterioration to low dielectric properties during further processing and applications.[76] Therefore, the development of flexible high-performance intrinsic low-k or ultralow-k polymer materials remains a great challenge in the microelectronics industry.

1.5 Objectives

Polybenzazoles are series of polymer material with high thermal stability, they are known as thermoresistant materials, such as fire-fight clothes. Most of the polybenzazoles are made from petroleum-based resources up to now. However, the fossil fuel is depleting with an increasing speed and will run out in tens of years, it is significant to explore the approaches to synthesize polybenzazoles for natural resources. In this research, natural bio-based resources are adopted to synthesize polybenzazoles with ultrahigh thermal resistance and excellent dielectric performance.

In chapter 1, copolymer polybenzimidazole-*co*-polybenzoxazole was synthesized via the copolymerization of 3,4-diaminobenzoic acid and 4-aimino-3-hydroxyl benzoic acid, which was obtained from bio-resources for the first time. The copolymers were synthesized with various composition and the thermal stabilities was characterized. Compared with the same copolymer synthesized from 3-amino-4-hydroxyl benzoic acid, the new synthesized one exhibited higher thermal stability.

In chapter 2, copolymer polybenzothiazoles was synthesized from bio-derived resources, which is the first time to successfully synthesize polybenzothiazoles from bio-derived monomer. the precursor monomer of the polymerization—4-amino-3-mercaptobenzoic acid was synthesized from bio derived 4-aminobenzoic acid through series of chemical

reactions. After copolymerized with 3,4-diaminobenzoic acid, copolymer polybenzothiazole-co-polybenzimidazole was obtained and showed excellent dielectric performance with a dielectric constant around 3 and a volume resistivity high that 10^{14} Ω/cm.

In chapter 4, terpolymer PBI-co-PBO-co-PA was designed and synthesized from bio derived monomers with ultrahigh thermal resistance and low dielectric constant. In the experiment, regular synthesis—simple polymerization of monomers failed to give a polymer that can be used to fabricate films, this problem was solved by stepwise polymerization of monomer: a prepolymerization of 3,4-diaminobenzoic acid and followed by the addition of 3-amino-4-hydroxyl benzoic acid and 4-aminobenzoic acid. The resulting polymers succeeded in film fabrication, ultrahigh thermal resistance and low dielectric constant were shown by the obtained films. The mechanism of the high thermal resistance was attributed to the appropriate incorporation of PA which enhanced the interchain interaction energy of hydrogen bonds according to the DFT calculation.

1.6 References:

1 M. G. A. Vieira, M. A. Da Silva, L. O. Dos Santos and M. M. Beppu, *Eur. Polym. J.*, 2011, 47, 254–263.

2 A. L. Andrady, *Mar. Pollut. Bull.*, 2017, **119**, 12–22.

3 Hisham A. Maddah, *Am. J. Polym. Sci.*, 2016, **6**, 1–11.

4 M. Khutia, G. M. Joshi, K. Deshmukh and M. Pandey, *Polym. Plast. Technol. Eng.*, 2015, **54**, 383–389.

5 T. Tanaka, G. C. Montanari and R. Mulhaupt, *IEEE Trans. Dielectr. Electr. Insul.*, 2004, **11**, 763–784.

6 Z. Deng, Y. Jiang, K. Chen, F. Gao and X. Liu, *Front. Microbiol.*, 2020, **11**, 353.

7 F. Leriche and J.-M. Zuliani, *Géographie, économie, société*, 2007, **9**, 19–38.

8 S. Becarelli, G. Siracusa, I. Chicca, G. Bernabei and S. Di Gregorio, *Water*, 2021, **13**, 3040.

9 Z. Liu, K. Wang, Y. Chen, T. Tan and J. Nielsen, *Nat. Catal.*, 2020, **3**, 274–288.

10 R. P. Babu, K. O'Connor and R. Seeram, *Prog. Biomater.*, 2013, **2**, 8.

11 J. Hildebrandt, A. Bezama and D. Thrän, *Waste Manag. Res. J. a Sustain. Circ. Econ.*, 2017, **35**, 367–378.

12 T. Garrison, A. Murawski and R. Quirino, *Polymers (Basel).*, 2016, **8**, 262.

13 A. Nag, M. A. Ali, M. Watanabe, M. Singh, K. Amornwachirabodee, S. Kato, T. Mitsumata, K. Takada and T. Kaneko, *Data Br.*, 2019, **25**, 104114.

14 T. P. Dawin, Z. Ahmadi and F. A. Taromi, *Prog. Org. Coatings*, 2018, **119**, 23–30.

15 J. Rajesh Banu, S. Kavitha, R. Yukesh Kannah, T. Poornima Devi, M. Gunasekaran, S.-H. Kim and G. Kumar, *Bioresour. Technol.*, 2019, **290**, 121790.

16 Z. N. Diyana, R. Jumaidin, M. Z. Selamat, I. Ghazali, N. Julmohammad, N. Huda and R. A. Ilyas, *Polymers (Basel).*, 2021, **13**, 1396.

17 S. P. Bangar, W. S. Whiteside, A. O. Ashogbon and M. Kumar, *Food Packag. Shelf Life*, 2021, **30**, 100743.

18 S. Esmaeilzadeh Saieh, H. Khademi Eslam, E. Ghasemi, B. Bazyar and M. Rajabi, *BioResources*, 2019, **14**, 5278–5287.

19 M. Mitrus, *Int. Agrophysics*, 2006, **20**, 31–35.

20 H. I. García-Cruz, M. R. Jaime-Fonseca, E. Von Borries-Medrano and H. Vieyra, *Rev. Mex. Ing. Química*, 2020, **19**, 395–412.

21 N. A. Faris, N. Z. Noriman, S. T. Sam, C. M. Ruzaidi, M. F. Omar and A. W. M. Kahar, *Appl. Mech. Mater.*, 2014, **679**, 273–280.

22 Z. Su, S. Huang, Y. Wang, H. Ling, X. Yang, Y. Jin, X. Wang and W. Zhang, *J. Mater. Chem. A*, 2020, **8**, 14082–14090.

23 D. W. Wei, H. Wei, A. C. Gauthier, J. Song, Y. Jin and H. Xiao, *J. Bioresour. Bioprod.*, 2020, **5**, 1–15.

24 C. T. Wood and M. Zimmer, *Appl. Soil Ecol.*, 2014, **77**, 72–79.

25 A. Nag, M. A. Ali, H. Kawaguchi, S. Saito, Y. Kawasaki, S. Miyazaki, H. Kawamoto, D. T. N. Adi, K. Yoshihara, S. Masuo, Y. Katsuyama, A. Kondo, C. Ogino, N. Takaya, T. Kaneko and Y. Ohnishi, *Adv. Sustain. Syst.*, 2020, **2000193**, 1–10.

26 H. Thai, C. Thuy Nguyen, L. Thi Thach, M. Thi Tran, H. Duc Mai, T. Thi Thu Nguyen, G. Duc Le, M. Van Can, L. Dai Tran, G. Long Bach, K. Ramadass, C. I. Sathish and Q. Van Le, *Sci. Rep.*, 2020, **10**, 909.

27 H. R. Bakhsheshi-Rad, Z. Hadisi, A. F. Ismail, M. Aziz, M. Akbari, F. Berto and X. B. Chen, *Polym. Test.*, 2020, **82**, 106298.

28 F. Garavand, M. Rouhi, S. H. Razavi, I. Cacciotti and R. Mohammadi, *Int. J. Biol. Macromol.*, 2017, **104**, 687–707.

29 G. A. Martău, M. Mihai and D. C. Vodnar, *Polymers (Basel).*, 2019, **11**, 1837.

30 E. Álvarez-Castillo, G. Caballero, A. Guerrero and C. Bengoechea, *J. Polym. Environ.*, 2021, **29**, 2789–2796.

31 W. A. Manamperi, J. D. Espinoza-Perez, D. M. Haagenson, C. A. Ulven, D. P. Wiesenborn and S. W. Pryor, *Ind. Crops Prod.*, 2015, **77**, 133–138.

32 B. Chalermthai, M. T. Ashraf, J.-R. Bastidas-Oyanedel, B. D. Olsen, J. E. Schmidt and H. Taher, *Polymers (Basel).*, 2020, **12**, 847.

33 K. Formela, L. Zedler, A. Hejna and A. Tercjak, *Express Polym. Lett.*, 2018, **12**, 24–57.

34 R. Dobrucka, *Logforum*, 2019, **15**, 129–137.

35 M. Dammak, Y. Fourati, Q. Tarrés, M. Delgado-Aguilar, P. Mutjé and S. Boufi,

Ind. Crops Prod., 2020, **144**, 112061.

36 A. Lappe, N. Jankowski, A. Albrecht and K. Koschorreck, *Appl. Microbiol. Biotechnol.*, 2021, **105**, 8313–8327.

37 K. P. Bye, V. Loianno, T. N. Pham, R. Liu, J. S. Riffle and M. Galizia, *J. Memb. Sci.*, 2019, **580**, 235–247.

38 N. Berezina, B. Yada and R. Lefebvre, *N. Biotechnol.*, 2015, **32**, 47–53.

39 R. Porta, *J. Appl. Biotechnol. Bioeng.*, 2017, **2**, 1111.

40 R. F. Al-Ghamdi, M. M. Fahmi and N. A. Mohamed, *Polym. Degrad. Stab.*, 2006, **91**, 1530–1544.

41 S.-A. Park, H. Jeon, H. Kim, S.-H. Shin, S. Choy, D. S. Hwang, J. M. Koo, J. Jegal, S. Y. Hwang, J. Park and D. X. Oh, *Nat. Commun.*, 2019, **10**, 2601.

42 S. W. Chuang, S. L. C. Hsu and Y. H. Liu, *J. Memb. Sci.*, 2007, **305**, 353–363.

43 S. Bourbigot and X. Flambard, *Fire Mater.*, 2002, **26**, 155–168.

44 *Int. J. Pharm. Res.*, , DOI:10.31838/ijpr/2021.13.01.245.

45 S. Sandell, J. Maire, E. Chávez-Ángel, C. M. Sotomayor Torres, H. Kristiansen, Z. Zhang and J. He, *Nanomaterials*, 2020, **10**, 670.

46 S. L. Malhotra, J. Hesse and L. P. Blanchard, *Polymer (Guildf).*, 1975, **16**, 81–93.

47 H. T. H. Nguyen, P. Qi, M. Rostagno, A. Feteha and S. A. Miller, *J. Mater. Chem. A*, 2018, 6.

48 L. Ozmen and T. A. G. Langrish, *Dry. Technol.*, 2002, **20**, 1177–1192.

49 P. Wang, L. Yang, S. Gao, X. Chen, T. Cao, C. Wang, H. Liu, X. Hu, X. Wu and S. Feng, *Adv. Compos. Hybrid Mater.*, 2021, **4**, 639–646.

50 S. J. Grabowski, *Crystals*, 2021, **11**, 1–21.

51 F. Kato, T. Sugimoto, K. Harada, K. Watanabe and Y. Matsumoto, *Phys. Rev. Mater.*, 2019, **3**, 112001.

52 S. Mehta, P. Agarwal, P. Shrivastava and J. Barlawala, *J. King Saud Univ. - Comput. Inf. Sci.*, 2022, **34**, 1466–1471.

53 D. Cao, L. Zhu, Z. Liu and W. Lin, *J. Photochem. Photobiol. C Photochem. Rev.*, 2020, **44**, 100371.

54 C. Feng, E. Sharman, S. Ye, Y. Luo and J. Jiang, *Sci. China Chem.*, 2019, **62**, 1698–1703.

55 S. Scheiner and M. Čuma, *J. Am. Chem. Soc.*, 1996, **118**, 1511–1521.

56 N. Yamaguchi, M. Mitome, A.-H. Kotone, M. Asano, K. Adachi and T. Kogure, *Sci. Rep.*, 2016, **6**, 20548.

57 K. L. Gordon, J. H. Kang, C. Park, P. T. Lillehei and J. S. Harrison, *J. Appl. Polym. Sci.*, 2012, **125**, 2977–2985.

58 F. Yao, W. Xie, M. Yang, H. Zhang, H. Gu, A. Du, N. Naik, D. P. Young, J. Lin and Z. Guo, *Mater. Today Phys.*, 2021, **21**, 100502.

59 M. Wuttig, *Phys. Status Solidi Basic Res.*, 2009, **246**, 1820–1825.

60 G. Lucovsky and R. M. White, *Phys. Rev. B*, 1973, **8**, 660–667.

61 L. J. Karas, C. Wu, R. Das and J. I. C. Wu, *WIREs Comput. Mol. Sci.*, , DOI:10.1002/wcms.1477.

62 M. Wuttig and S. Raoux, *Zeitschrift fur Anorg. und Allg. Chemie*, 2012, 638.

63 R. A. Laskowski, D. S. Moss and J. M. Thornton, *J. Mol. Biol.*, 1993, **231**, 1049–1067.

64 L. Glasser, *J. Appl. Crystallogr.*, 2020, **53**, 1101–1107.

65 G. J. Linker, P. T. Van Duijnen and R. Broer, *J. Phys. Chem. A*, 2020, **124**, 1306–1311.

66 M. Pechlaner, A. P. Dorta, Z. Lin, V. H. Rusu and W. F. van Gunsteren, *J. Comput. Chem.*, 2021, **42**, 418–434.

67 G. Maier, *Prog. Polym. Sci.*, 2001, **26**, 3–65.

68 M. Lin and Y. C. King, *IEEE Trans. Device Mater. Reliab.*, 2021, **21**, 207–214.

69 W. Abdelmoez and H. Yoshida, *Biotechnol. Prog.*, 2008, **24**, 466–75.

70 X. Wang, J. Li, F. Li, Y. Pan, D. Cai, D. Mao, L. Chen and S. Luan, *Front. Plant Sci.*, 2021, **12**, 730002.

71 J. Y. Wang, S. Y. Yang, Y. L. Huang, H. W. Tien, W. K. Chin and C. C. M. Ma, *J. Mater. Chem.*, 2011, **21**, 13569–13575.

72 J. B. Wade, J. Liu, R. Coleman, P. Richard Grimm, E. Delpire and P. A. Welling, *Am. J. Physiol. - Ren. Physiol.*, 2015, **308**, F923–F931.

73 W. Wang, G. Ren, M. Zhou and W. Deng, *Polymers (Basel).*, 2021, **13**, 1075.

74 B. Wang, G. Liang, Y. Jiao, A. Gu, L. Liu, L. Yuan and W. Zhang, *Carbon N. Y.*, 2013, **54**, 224–233.

75 X. Y. Zhao and H. J. Liu, *Polym. Int.*, 2010, 59, 597–606.

76 M. W. Ahmad, B. Dey, G. Sarkhel, D. S. Bag and A. Choudhury, *J. Mol. Struct.*, 2019, **1177**, 491–498.

Chapter II

Syntheses and characterization of bio-based poly{benzoxazole-*co*-benzimidazole} with high thermal resistance

Chapter II

2.1 Introduction

Bio-based plastics with high performance is of great significance for environmental sustainability.[16,78] Fossil fuel-based polybenzimidazole is well known as commercially available material Celazole®, having ultrahigh thermal stability and mechanical performance.[9] 2,5-polybezimidazole (PBI), a polybenzazole has the similar structure with Celazole® is synthesized from precursor monomer 3,4-diaminobenzoic acid (DABA) which can be obtained by the modification of 3-amino-4-hydroxylbenzoic acid (3,4-AHBA) derived from *Streptomyces griseus*.[79] Bio-based PBI shows outstanding thermal resistance with a 10% weight loss temperature higher than 700 ℃, however, PBI fails to present an outstanding dielectric performance due to the conductive imidazole rings which have high polarizability.[80]

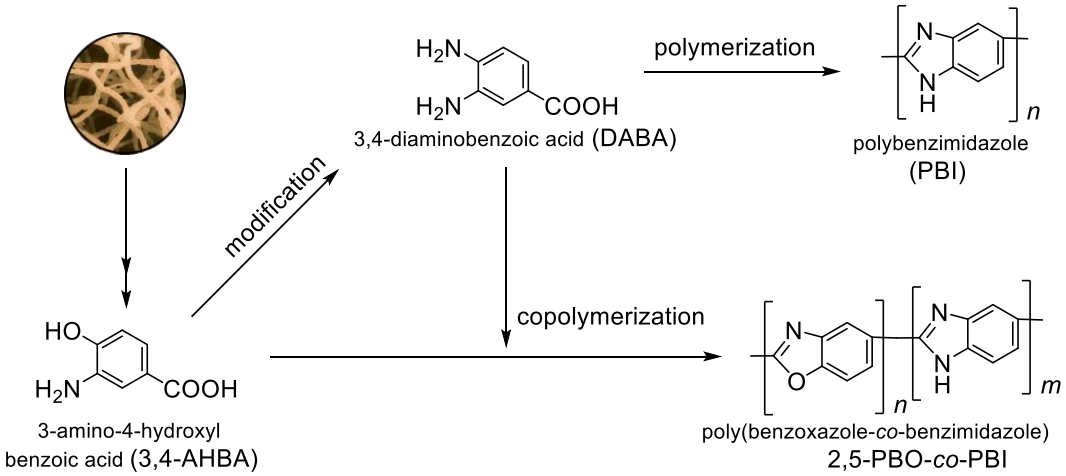

Figure 2.1. Synthetic routine of PBI and its copolymer PBO-*co*-PBI.

To solve this problem, 2,5-polybenzoxazole (2,5-PBO) is introduced into PBI backbone to form copolymer 2,5-PBO-*co*-PBI through the copolymerization of DABA and 3,4-AHBA (**Figure 2.1**).[79] The utilization of non-polar ring-type linkages to connect the aromatic rings is the strategy to design the molecular with low dielectric constant (low-*k*). PBO have a structure containing aromatic heterocycles, which have no polar functional groups or active protons on the structure, it is hence intended as perfect low-*k* material. 2,5-PBO-*co*-PBI has relatively lower structural polarizability than PBI and

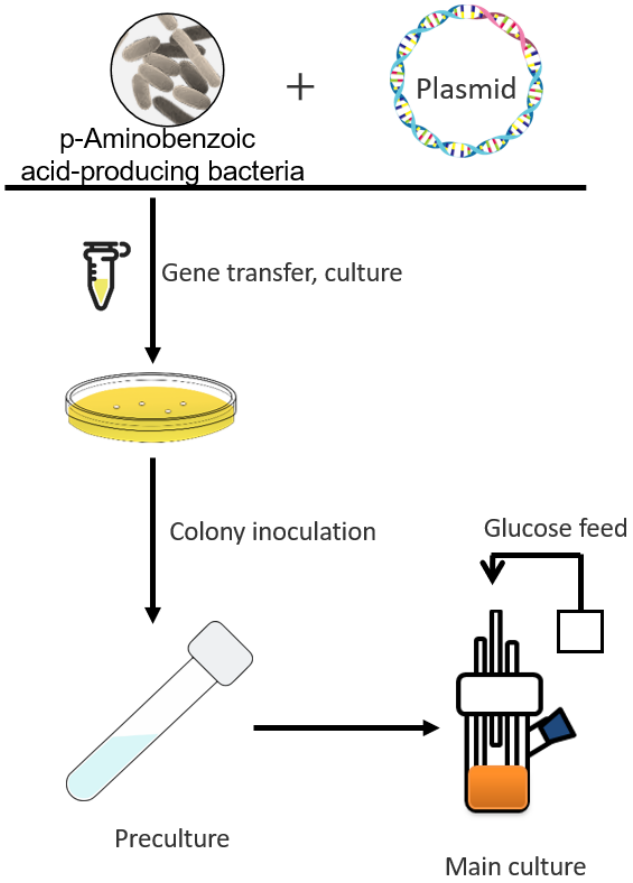

Figure 2.2. The production of 4,3-AHBA (performed in KAO company).

therefore present a dielectric constant of approximately 2 to 3, this is an excellent dielectric performance prior to most of material available in the market. However, due to the incorporation of 2,5-PBO, the copolymer showed a weakened thermal stability compared with PBI, making the copolymer inferior in thermoresistance.[79,81–83] Therefore, it is important to find approaches to optimize the thermal stability of 2,5-PBO to make a highly thermostable copolymer.

A monomer 4-amino-3-hydroxyl benzoic acid (4,3-AHBA) provide by KAO company offers an approach to solve the problem (**Figure 2.2**). 4,3-AHBA is the precursor monomer of 2,6-polybenzoxazole (2,6-PBO), which has an analogous structure with 2,5-PBO, can be used to copolymerize with DABA and synthesize copolymer 2,6-PBO-*co*-PBI, in spite of the similar structure, the difference in heterocycles is worthy to explore.

2.2 Experimental section

2.2.1 Materials

AHBA (purity: > 97%) in both types were purchased from TCI, 4,3-AHBA is partially provided by KAO company. DABA (purity: 98%), 4-aminobenzoic acid (PABA) (purity: > 99%), sodium hydroxide (NaOH) (purity: > 98%) were purchased from TCI (Tokyo Chemical Industry). Poly (phosphoric acid) (PPA) (purity: 85%) was obtained

from Sigma-Aldrich. Methane sulfonic acid (MSA) (purity: > 98%) and trifluoroacetic acid (TFA) (purity: > 98%) were supplied by Wako pure chemical Industries, Ltd. pH test paper, supplied by Macherey-Nagel GmbH & Co. KG, Düren, Germany). Copper wire were purchased from SENKO Co., Ltd. All the solvents and reagents in this research were used as received without any further processing or purification.

2.2.2 Syntheses

2.2.2.1 Monomers

AHBA (6.0g, 39.2 mmol) was dispersed in 30 mL methanol and kept stirring. Hydrochloric acid (12 N) was added drop wise to the suspension until DABA was completely dissolved, after the color changed from pink to dark red, kept stirring at room temperature for 4 h. The yellow salt of AHBA dihydrochloride (AHBA·HCl) was obtained *via* solvent evaporation (yield: (5.4g, 94%). AHBA hydrochloride (AHBA·HCl) salt were obtained following the same method as of AHBA.

2.2.2.2 Homopolymers

2,6-PBO, 2,5-PBO homopolymer and 2,6-PBO-co-2,5-PBO copolymer were synthesized through the polycondensation in polyphosphoric acid (PPA) as shown in **Scheme 2.1**, **Scheme 2.2** and **Scheme 2.3**. The preparation of 2,6-PBO was described blow as a representative synthetic procedure. 25 g of PPA was taken to a three-necked

round-bottomed flask with a magnetic stirrer and heated at 100 °C for 1 h in a nitrogen gas atmosphere to remove any traces of moisture. Subsequently, AHBA·HCl (1134.0 mg, 6.00 mmol) was added to the flask, and the contents were stirred continuously for 1 h until all the moisture was eliminated, and the monomeric solids were completely dissolved in the reaction system. The mixture was then successively heated at 160 °C, 180 °C, and 200 °C for 4 h each, and ultimately at 220 °C for 12 h, during which the color of the solution changed from red to dark brown. The resultant solution was dispersed in water and stirred for 12 h to remove PPA; subsequently, a brown solid was obtained on filtration. After drying under vacuum, the solid was ground into a powder and suspended in deionized water. Then, 1M NaOH was slowly added, and the solution was stirred until the pH of the solution reached 7.0, and it was maintained for 1 h. The solid was collected by filtration and dried under vacuum to obtain a brown powder (601.8 mg, 5.4 mmol) as the final product with a yield of 85%.

2.2.2.3 Copolymers

The copolymers were synthesized via the copolymerization of 4,3-AHBA and DABA, Molar compositions (mol%) of PBO-PBI are 10-90, 20-80, 30-70, 40-60, 50-50 and 60-40, respectively. The synthetic methods are the same as the preparation of PBO

homopolymers. The synthesis of the PBO-*co*-PBI in the composition (mol%) of 20-80 is described below as a representative synthetic procedure (**Scheme 2.4**). Herein, 25 g of PPA was taken to a three-necked round-bottomed flask with a magnetic stirrer and heated at 100 °C for 1 h in a nitrogen gas atmosphere to remove any traces of moisture. Subsequently, AHBA·HCl (226.8 mg, 1.20 mmol), DABA ·HCl (1080.0 mg, 4.80 mmol) were added to the flask, and the contents were stirred continuously for 1 h until all the moisture was eliminated, and the monomeric solids were completely dissolved in the reaction system. The mixture was then successively heated at 160 °C, 180 °C, and 200 °C for 4 h each, and ultimately at 220 °C for 12 h, during which the color of the solution changed from red to dark brown. The resultant solution was dispersed in water and stirred for 12 h to remove PPA; subsequently, a brown solid was obtained on filtration. After drying under vacuum, the solid was ground into a powder and suspended in deionized water. Then, 1M NaOH was slowly added, and the solution was stirred until the pH of the solution reached 7.0, and it was maintained for 1 h. The solid was collected by filtration and dried under vacuum to obtain a brown powder (621.0 mg, 5.4 mmol) as the final product with a yield of 89%. An analogous synthetic process was performed for 2,5-PBO-*co*-PBI copolymers (**Scheme 2.5)** and each of the 2,6-PBO-*co*-PBI with other molar ratios.

2.2.3 Film fabrication

100 mg PBO-co-PBI (mol%: 20-80) was dispersed in 3 mL TFA and 2 drops of MSA mixture solution. After stirring at 60 degree for 24 hours, the copolymer completely dissolved in the acid and form a dark brown solution. The solution was taken by dropper and distributed in silicon plate homogenously and dry at room temperature for 12 h to evaporate the TFA.

Subsequently, the dried film was put in water for 12 h to remove the resident MSA. Finally, the film was taken out from water and sandwiched by silicon plate and dried under vacuum for 12 h to obtain a brown film

2.2.4 Measurements

Fourier transform infrared (FT-IR) spectra of terpolymers were recorded in a Perkin-Elmer Spectrum with a diamond-attenuated total reflection (ATR) accessory. The wavenumber range was set as 4000 to 400 cm^{-1}. Solid-state ^{13}C NMR CP/TOSS (Total Suppression of Spinning Sidebands) spectra of the terpolymer were recorded with a Bruker Advance III spectrometer operating at 500 MHz. Terpolymer samples were filled into 7 mm diameter zirconia rotor with a Kel-F cap and then spun at 8 kHz. The contact time and the period between successive accumulations were set as 2 s and 5s respectively. The total number of the scans was set as 25000.

Thermo-gravimetric analysis (TGA) curves of the terpolymers were recorded using a HITACHI STA7200. In a platinum crucible, the samples (5mg) were placed and heated under a nitrogen atmosphere to 800 °C with a heating rate of 10 °C/min. The 5% mass loss temperature (T_{d5}) and 10% mass loss temperature (T_{d10}) of the samples were taken as indices of the thermal decomposition temperatures.

The stress-stain curves of the terpolymers were recorded *via* tensile mode mechanical tests using an Instron-3365 mechanical tester instrument at room temperature. Samples were shaped into a rectangular film with a length of 40 mm, width of 7 mm and a thickness of 15 μm. The elongation speed was set as 0.4 mm/min.

2.3 Result and discussions

2.3.1 PBOs comparisons:

Homopolymer 2,5-PBO and 2,6-PBO were synthesized from 3,4-AHBA and 4,3-AHBA respectively, copolymer of them was also synthesized as a reference for the comparison. The synthetic routines are listed as follows.

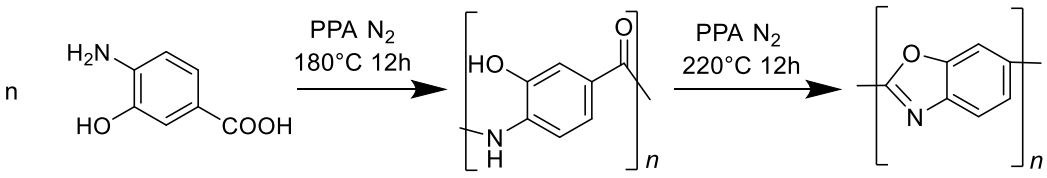

Scheme 2.1. Synthetic pathway of homopolymer 2,6-PBO.

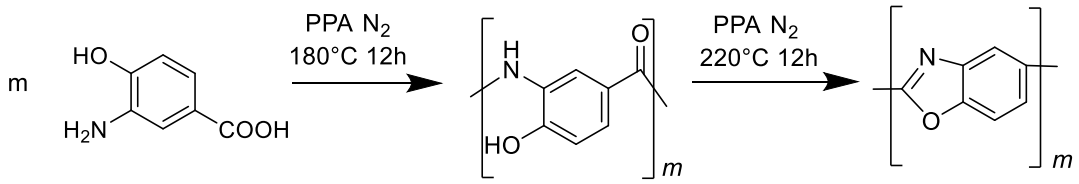

Scheme 2.2. Synthetic rout of homopolymer 2,5-PBO.

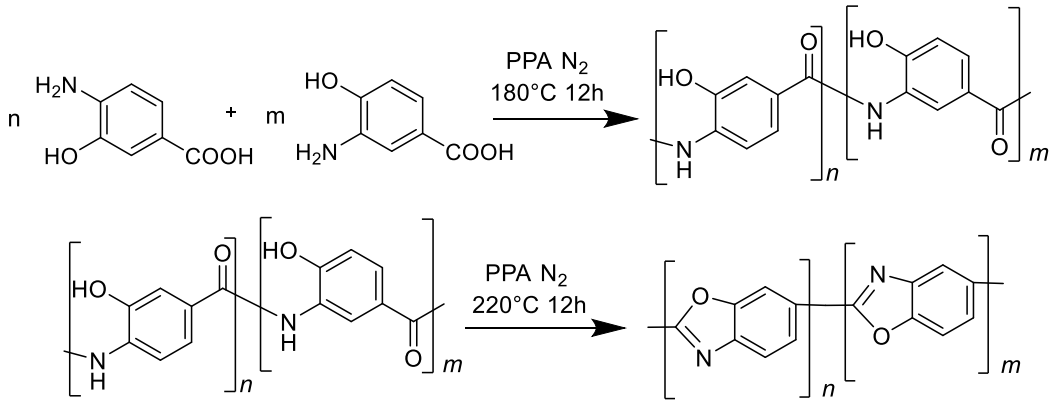

Scheme 2.3. Synthetic rout of 2,6-PBO-co-2,5-PBO

Table 2.1. Thermal decomposition temperatures of PBOs.

	T_{d5} (℃)	T_{d10} (℃)
2,5-PBO	651	675
2,6-PBO	651	671
Copolymer PBO	651	671

The resulting polymers were characterized the thermal stability in TGA, as is shown in **Table 2.1** and **Figure 2.3.** All the polymers show a T_{d5} of 651 ℃ and the T_{d10} around 670 ℃, indicating the PBO of 2 types have the similar thermal stability.

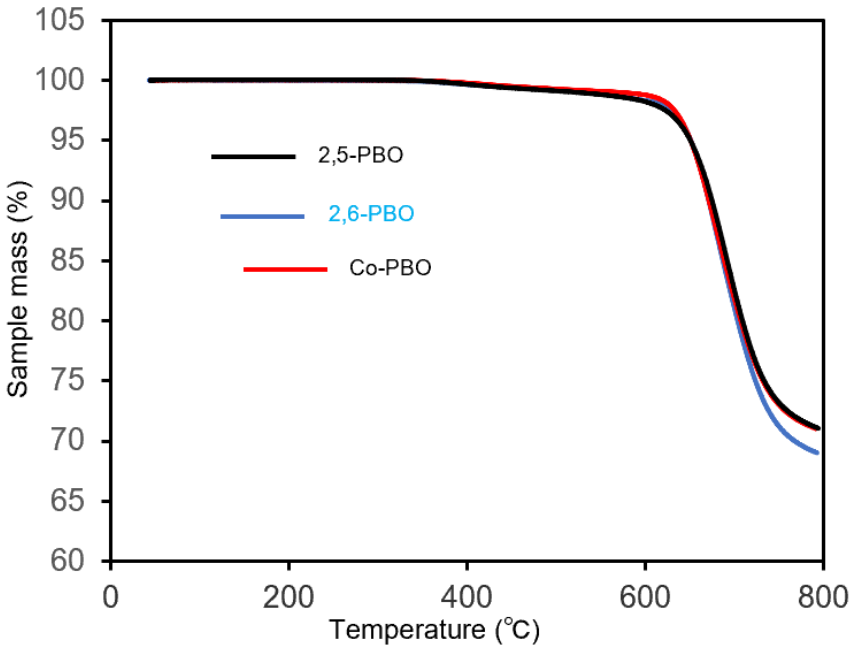

Figure 2.3. TGA curves of PBOs.

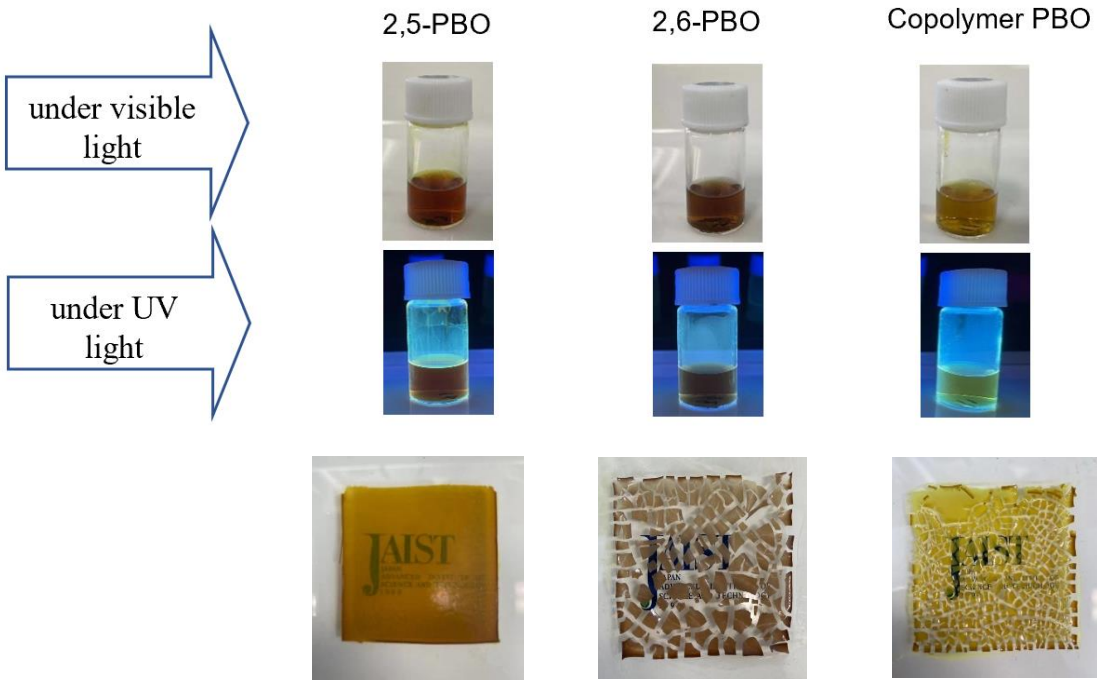

Figure 2.4. The film images of PBOs.

2,5-PBO, 2,6-PBO and their copolymer were checked the solubility in various solvents.

3 kinds of polymer exhibit completely the same solubility according to the result (**Table**

Table 2.2. The result of solubility measurement of PBOs.

	DMSO	DMAc	DCM	H_2SO_4	Formic acid	TFA	MSA	TFA MSA	Formic acid TFA
2,6-PBO	-	-	-	+	+ -	+ -	+	+	+
2,5-PBO	-	-	-	+	+ -	+ -	+	+	+
Copolymer PBO	-	-	-	+	+ -	+ -	+	+	+

+ soluble +/- Partially soluble - insoluble

2.2). They are completely insoluble in regular organic solvent, but soluble in strong acid, interestingly, they are partially soluble in formic acid, making it possible to fabricate film without strong acid.

Film fabrications were conducted with formic acid or TFA as solvent. 2,6-PBO is successfully fabricated into film but too brittle to scratch form the plate, 2,5-PBO and copolymers failed to fabricate a complete film, which split into fragments after the solvent is dried. All type of PBOs are hard to be casted into a pliable film, indicating they are almost impossible to characterize film properties or be utilized in any applications. Therefore, it is important to explore the approach to make a polymer able to be fabricated into film.

2.3.2 Copolymer PBO-*co*-PBI

In order to fabricate a ductile film, 4,3-AHBA and 3,4-AHBA was copolymerized with DABA, to synthesize copolymer 2,6-PBO-co-PBI and 2,5-PBO-co-PBI, respectively. The synthetic routines are shown as below:

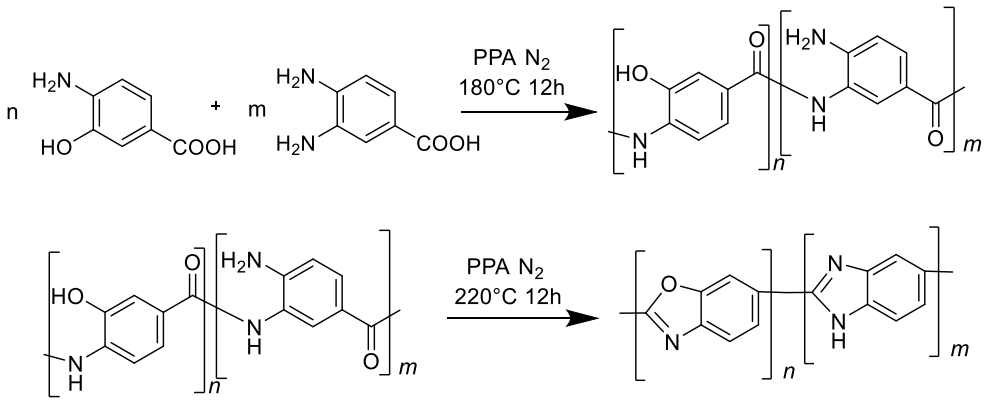

Scheme 2.4. The synthetic routine of copolymer 2,6-PBO-*co*-PBI.

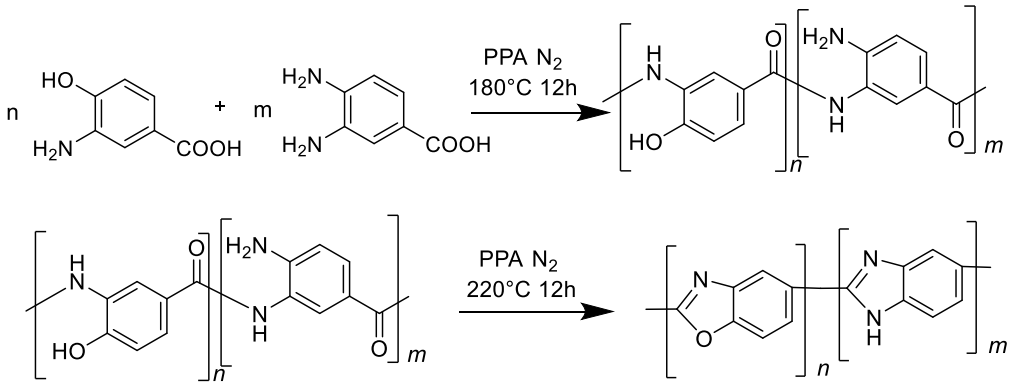

Scheme 2.5. The synthetic routine of copolymer 2,5-PBO-*co*-PBI.

The copolymer 2,6-PBO-co-PBI in serval compositions were fabricated into films, the images of film are shown in **Figure 2.5,** judging from the film state, the film durability decreases with the increasing amount of 4,3-AHBA incorporated into the copolymers, when PBO amount is lower than 20% in the mol composition, ductile film can be

obtained. A complete film cannot be fabricated if the 4,3-AHBA composition is higher than 50%.

The synthesized copolymers (2,6-PBO-*co*-PBI and 2,5-PBO-*co*-PBI) were further compared in thermal stabilities. their 5% and 10% thermal decomposition temperature were taken as the index of the stability (**Table 2.1**). Interestingly, the copolymer 2,6-PBO-*co*-PBI showed a relatively higher thermal stability than copolymer 2,5-PBO-*co*-PBI, this is completely different from the situation of PBO homopolymers (**Figure 2.2**). According to the data obtained, in the same molar compositions, 2,6-PBO-*co*-PBI showed a significant higher T_{d10} and T_{d5} values.

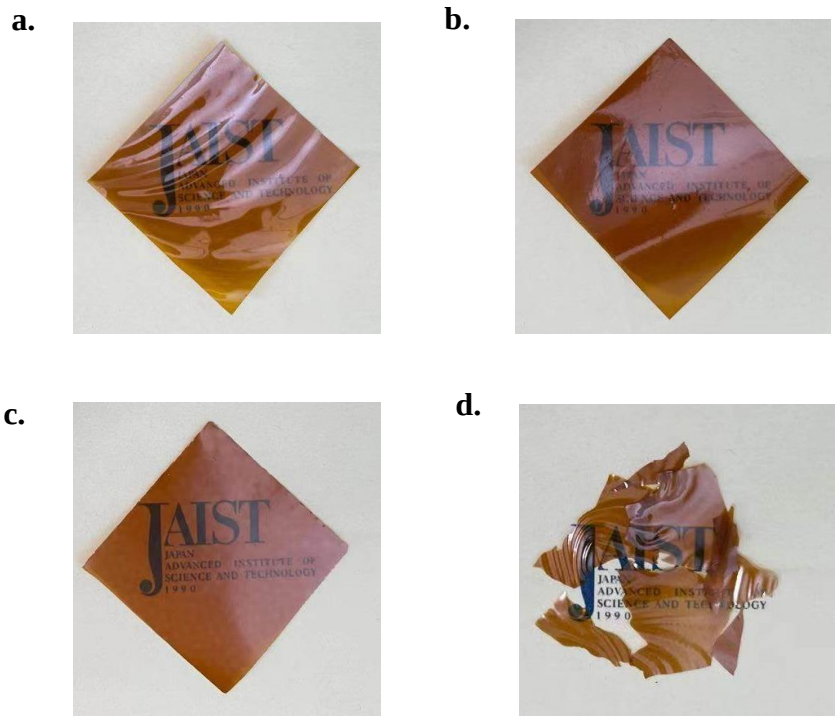

Figure 2.5. The film images of copolymer 2,6-PBO-*co*-PBI in various composition (mol %): **a.** 10/90; **b.** 20/80; **c.**40/60; **d.** 50/50.

Table 2.3. T_{d5} and T_{d10}values of 2 copolymers.

	2, 6-PBO-*co*-PBI		2, 5-PBO-*co*-PBI	
PBO ratios	T_{d5} (°C)	T_{d10}(°C)	T_{d5}(°C)	T_{d10}(°C)
10	638	653		
20	613	696	601	664
30	640	742		
40	620	668	593	640
50	612	666	574	614
60	599	649	578	613

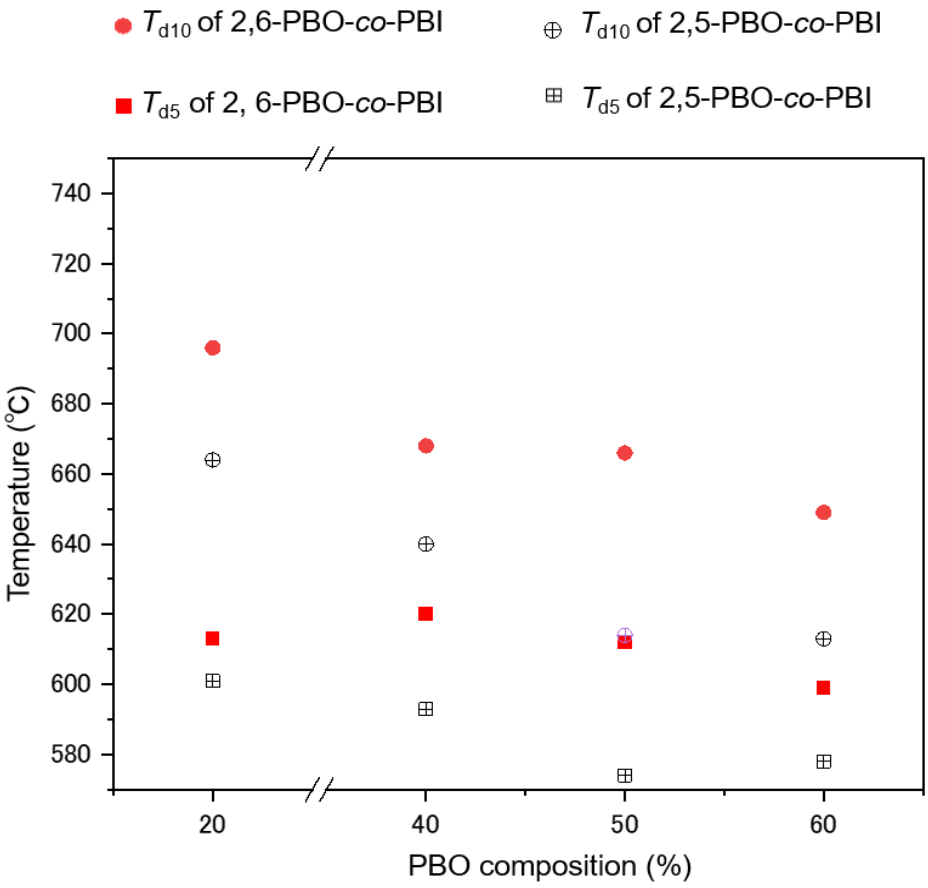

Figure 2.6. Comparison of thermal decomposition temperatures of 2,6-PBO-*co*-PBI and 2,5-PBO-*co*-PBI.

2.4 Conclusion

Homopolymer 2,5-PBO and 2,6-PBO and their copolymer with PBI were synthesized from bio-derived monomers 3,4-AHBA and 4,3-AHABA. There is no significant difference in thermal stability between the homopolymers, both types of PBO showed a T_{d5} of 651 ℃ and T_{d10} of approximately 671 ℃. However, after copolymerized with PBI, an obvious difference in thermal decomposition temperatures occurred between the 2 types of copolymers. 2,6-PBO-co-PBI exhibit higher thermal stability than another copolymer. The films were successfully fabricated by the copolymer 2,6-PBO-co-PBI, and the higher molar composition of PBI tends to present more durable film.

2.5 References:

1 M. Rayung, M. M. Aung, S. C. Azhar, L. C. Abdullah, M. S. Su'ait, A. Ahmad and S. N. A. M. Jamil, *Materials (Basel).*, 2020, **13**, 838.

2 Z. N. Diyana, R. Jumaidin, M. Z. Selamat, I. Ghazali, N. Julmohammad, N. Huda and R. A. Ilyas, *Polymers (Basel).*, 2021, **13**, 1396.

3 Z. Liu, K. Wang, Y. Chen, T. Tan and J. Nielsen, *Nat. Catal.*, 2020, **3**, 274–288.

4 A. Nag, M. A. Ali, M. Watanabe, M. Singh, K. Amornwachirabodee, S. Kato, T. Mitsumata, K. Takada and T. Kaneko, *Polym. Degrad. Stab.*, 2019, **162**, 29–35.

5 A. Nag, M. A. Ali, M. Watanabe, M. Singh, K. Amornwachirabodee, S. Kato, T. Mitsumata, K. Takada and T. Kaneko, *Data Br.*, 2019, **25**, 104114.

6 K. Fukukawa, Y. Shibasaki and M. Ueda, *Macromolecules*, 2004, **37**, 8256–8261.

7 T. Kuroki, Y. Tanaka, T. Hokudoh and K. Yabuki, *J. Appl. Polym. Sci.*, 1997, **65**, 1031–1036.

8 B. D. Freeman, D. R. Paul, K. Czenkusch, C. P. Ribeiro, C. Ba, C. P. Ribeiro Jr. and C. Ba, *U.S. Pat. Appl. Publ.*, 2012, **1**, 63.

Chapter III

High performance low-*k* poly{benzothiazole-*co*-benzimidazole} bio-plastic showing high thermal stability

Chapter III

3.1 Introduction

Bio-polybenzazoles are series of polymers with high thermomechanical performance.[84,85] Polybenzazoles possess a highly conjugated backbone constructed by benzene rings and hetero rings, endow the polymers strong molecular stability. Conventional polybenzimidazoles and are well known as highly commercial thermoplastic material celazole and Zylon, respectively, in the market.[25,43] In our laboratory, 2,5-polybenzimidazole (PBI) and 2,5-polybenzoxazole (PBO) are synthesized using monomers derived from bio resources, they have analogous structures with celazole and Zylon but exhibit prior thermal resistance than conventional celazole PBIs and Zylon PBOs. However, both polymers show drawbacks due to the structures. PBI present a 10% weight loss temperature higher than 700 degrees, but its dielectric constant is characterized higher than 3.2,[79] which is too high to be utilized as thermal insulating material, this is because the imidazole rings have secondary amine in its structure, the proton on the secondary amine make the structure conductive.[13] In contrast, PBO shows low dielectric constant because of the low structural polarizability because of the existence of oxazole rings in the backbone, but PBO tend to present a relatively lower thermal stability in comparison with PBI, the 10% weight loss

temperature about 600 ℃, which makes it inferior in thermoresistant materials.[82] Therefore, it is significant to explore a new polymer with novel structure integrating both thermal stability an d dielectric performance.

As a member of polybenzazoles, polybenzothiazole (PBT) is not well investigated so far due to the low applicability that PBT polymer is hard to be used to fabricate a film.[83,86] PBT has the analogous molecular structure with PBO, but significant difference occurs between them due to the thiazoles. Thiazoles are member of the azoles, heterocycles that include imidazoles and oxazoles.[87,88] Thiazole is a functional group, oxazoles are related compounds, with sulfur replaced by oxygen. Thiazoles are also structurally similar to imidazoles, with the thiazole sulfur replaced by nitrogen. Thiazole rings are planar and aromatic, they are characterized by larger pi-electron delocalization than the corresponding oxazoles and have therefore greater aromaticity. This aromaticity cab be evidenced by the chemical shift of the ring protons in proton NMR spectroscopy, showing a stronger diamagnetic ring current. Considering the higher aromaticity brings stronger structural resonance,[61] which results higher stability, PBT polymer can be expected greater thermal stability than PBO. Besides, compared with PBI, the structure of PBT has lower polarizability due to the absence of proton in thiazole rings, PBT can theoretically be expected to show lower dielectric constant.[25] Therefore, PBT is

synthesized as a polymer integrated both low dielectric constant and high thermal resistance.

In this research, PBT is synthesized from bio monomers and its copolymers with PBI is synthesized. The resulting copolymers present a high thermal stability as well as high elongation after light modifications.

3.2 Experimental section

3.2.1 Materials

The following reagents was used: 3, 4-AHBA, was purchased (TCI Tokyo, Japan). Methanol, acetone, hexane, trifluoroacetic acid (TFA), N, N-dimethylacetamide (DMAc), potassium dichromate (K_2CO_3), potassium hydroxide (KOH), hydrochloric acid (HCl), methanesulfonic acid (Me_3SO_3H), phosphorus(V)oxide (P_2O_5), sulfuric acid (H_2SO_4), dimethylsulfoxide (DMSO) and dimethylsulfoxide/d6 (NMR solvent) were purchased from Kanto chemicals Co. Inc. Palladium-charcole(5%) from Sigma-Aldrich Polyhosphoric acid (PPA), 2-bromoisobutylamide, and 3, 4-diaminobenzoic acid (3,4-DABA) were purchased from TCI (Tokyo, Japan). All the chemicals were used for their particular purpose as received.

3.2.2 Synthesis of monomers

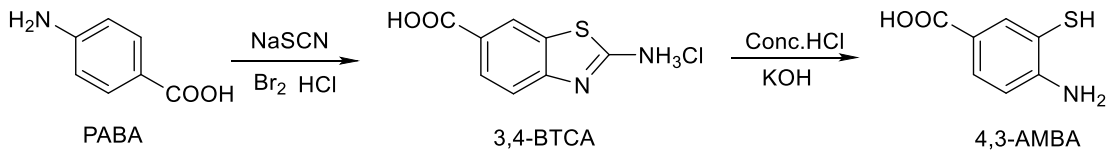

Scheme 3.1. synthesis of monomer 4-amino-3-mercaptobenzoic acid （AMBA）from bio-based para aminobenzoic acid.

AMBA was synthesized though the synthetic pathway shown in **Scheme 3.1.** 4-aminobenzoic acid (274 mg, 2 mol) and NaSCN（178.4 mg，2.2 mmol）were added to a 100-mL round bottled flask and degassed to remove the moisture, after degassed, inside the bottle was kept nitrogen gas atmosphere, then, methanal (10mL) was added to the flask using a syringe to dissolve ABA and NaSCN, the reaction system was cooled to −5 °C and added bromine (35mg, 2.2 mmol) was added dropwise. The reaction mixture was kept stirring for 2 h and then filtered to obtain a white precipitate. The precipitate was then washed by water to form a white solid. Subsequently, the solid was heated and refluxed in HCl solution (15mL, 1M) for 1 h, filtered while hot to give a clear solution, to the solution was added concentrated hydrochloric acid (5 mL). ultimately, the resulting solution was placed in a refrigerator to form a white precipitate, after filtration, white solid was obtained.

KOH (41 g, 0.73 mol) was dissolved in water (60 mL), and then added to the product of the previous step (31 g, 0.14 mol), heated to reflux at temperature of 130–135 °C; after

cooling, concentrated hydrochloric acid (approximately 45 mL) was added into the mixture, and placed in the refrigerator for 30 min, filtered, then washed with water to give the crude product, which was recrystallized from methanol to give pure yellowish target product.

3.2.3 Polymer syntheses

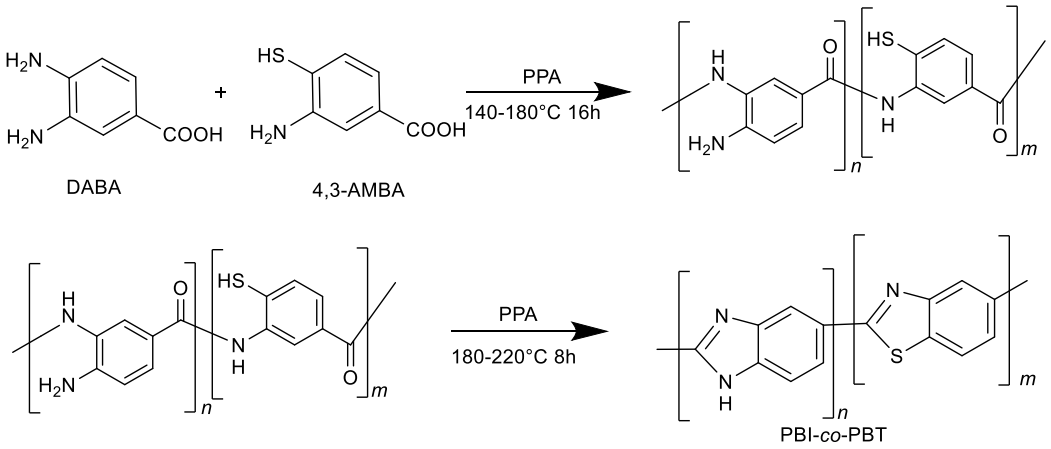

Scheme 3.2. Synthetic routine of copolymer PBT-*co*-PBI.

The PBT-*co*-PBI molar compositions are 90%-10%, 80%-20%, 70%-30%, 60%-40% and 50%-50% respectively. The synthesis of copolymer with a molar ratio of 80%-20% was described as a representative synthetic procedure (**Scheme 3.2**). Herein, 30 g of PPA was added to a 3-necked round-bottomed flask with a magnetic stirrer and heated at 100 °C for 1 h in a nitrogen gas atmosphere to remove any traces of moisture. Then, DABA (1080 mg, 4.8 mmol) and AMBA (203 mg, 1.2mmol) were added to the flask and keep stirring for 1 h to remove the eliminate the moisture. After the monomeric solids were completely dissolved in the reaction system, the mixture was then

successively heated at 180 °C, and 200 °C for 6 h each, and ultimately at 220 °C for 12 h, during which the color of solution turned from red to dark brown, the viscosity increased significantly. The mixture was dispersed in water and continuously stirred for 12 h to remove the PPA. Subsequently, the mixture was filtered to obtain a brown solid, the resultant solid was ground into powder and dispersed into deionized water. Then, 1M NaOH was added to the solution dropwise while stirring until the pH reach 7.0. Finally, after filtration and dried under vacuum, a solid (808 mg) with a dark yellow color was obtained with a yield of 83%. The copolymers of other molar ratios were synthesized using an identical method.

3.2.4 Film fabrication

The cast of PBI-*co*-PBT (100.0 mg, 0.3 mmol) was made over TFA solution (2 mL) containing 1 drop of MSA on a silicon substrate. After drying at 25 °C, the film was scratched off the substrate and then immersed in deionized water for 24 h to remove the residual acid. The self-standing film was successfully fabricated, and the film was further dried at 80 °C for 12 h.

3.2.5 Measurements

Fourier transform infrared (FT-IR) spectra of terpolymers were recorded in a Perkin-Elmer Spectrum with a diamond-attenuated total reflection (ATR) accessory. The wavenumber range was set as 4000 to 400 cm^{-1}. Solid-state ^{13}C NMR CP/TOSS (Total

Suppression of Spinning Sidebands) spectra of the terpolymer were recorded with a Bruker Advance III spectrometer operating at 500 MHz. Terpolymer samples were filled into 7 mm diameter zirconia rotor with a Kel-F cap and then spun at 8 kHz. The contact time and the period between successive accumulations were set as 2 s and 5s respectively. The total number of the scans was set as 25000.

The viscosity of terpolymer was measured through a viscometer SIBATA 026300-3. Conc. sulfuric acid (H_2SO_4) was used as a solvent. Thermo-gravimetric analysis (TGA) curves of the terpolymers were recorded using a HITACHI STA7200. In a platinum crucible, the samples (5mg) were placed and heated under a nitrogen atmosphere to 1000 °C with a heating rate of 10 °C/min. The 5% mass loss temperature (T_{d5}) and 10% mass loss temperature (T_{d10}) of the samples were taken as indices of the thermal decomposition temperatures.

The stress-stain curves of the terpolymers were recorded *via* tensile mode mechanical tests using an Instron-3365 mechanical tester instrument at room temperature. Samples were shaped into a rectangular film with a length of 40 mm, width of 7 mm and a thickness of 15 μm. The elongation speed was set as 0.4 mm/min.

The electrical resistivity of the terpolymer films was measured using a digital megohmmeter (DSM-8104 HIOKI) at 25 °C. External electromagnetic noise was

shielded by a Faraday cage during the measurement. Through conductive rubber electrodes with a guard electrode, two terminal methods were adopted to apply 1kV DC electric voltage to the film which had dimensions of 40×40 mm. The formula $\rho_v = (S/t) \times R_m$ was used to calculate the volume resistivity ρ_v (Ω cm), where S is the area of the electrode, t represents the thickness of the film.

The crystallinity was investigated using an X-ray diffractometer (SmartLab; Rigaku Corp., Akishima, Japan). Wide-angle X-ray diffraction (WAXD) patterns was checked from the facade of the film with a graphite-moznochromatized Cu Kα radiation beam generated at 100 mA and 40 kV.

The measurement of dielectric constant of the terpolymer films were carried out in an LCR meter (HIOKI IM3536) at 20 °C with a frequency of 1 MHz. The measurement was carried out by two terminals method with an applied electric potential of 1.0 V. The film was sandwiched between two electrodes with a constant pressure of 86 kPa and the sample holder was set in a Faraday cage. The relative dielectric constant (k_r) was calculated via the formula of $k_r = Cd/k_0A$, where C is the capacitance, d is thickness of film, A is the cross-sectional area of film and k_0 is the dielectric constant in vacuum ($=8.854\times10^{-12}$ F/m).

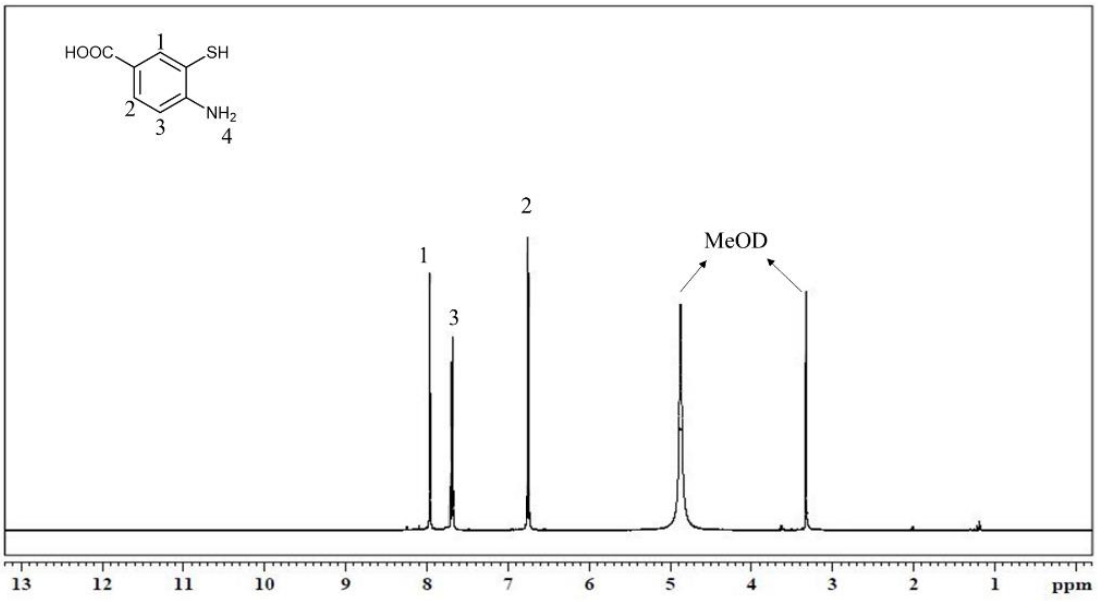

Chemical shift (ppm)

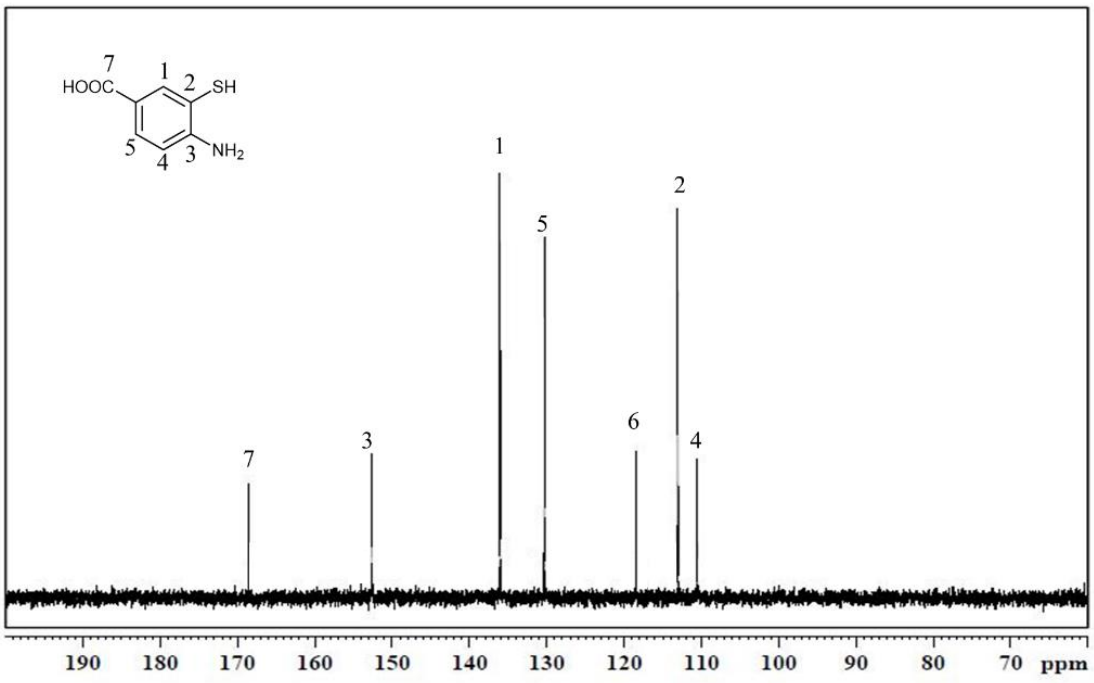

Chemical shift (ppm)

Figure 3.1. [1] H NMR (upper) and [13]C NMR (Lower)spectroscopy of AMBA (solvent: MeOD-d_4).

3.3 Result and Discussions

3.3.1 Structure confirmation

Monomer AMBA is successfully synthesized and the structure is confirmed by ^{1}H proton NMR and ^{13}C NMR. All the peaks are perfectly attributed in both spectroscopy.

The structure of PBT-co-PBI is confirmed by ^{13}C solid-state NMR (CPTOSS). The measurement of copolymer in composition (mol%) is taken a representative of the copolymer in all mol compositions. All the signals appear with in the chemical shift of 40 to 200 ppm as is shown in **Figure 3.2**. The signal in 95 ppm is attributed to the benzene ring carbons of the PBI and PBT, so are the broad signal in about 116 ppm. The signal in approximately 148 ppm is attributed to the benzene carbons bonded with

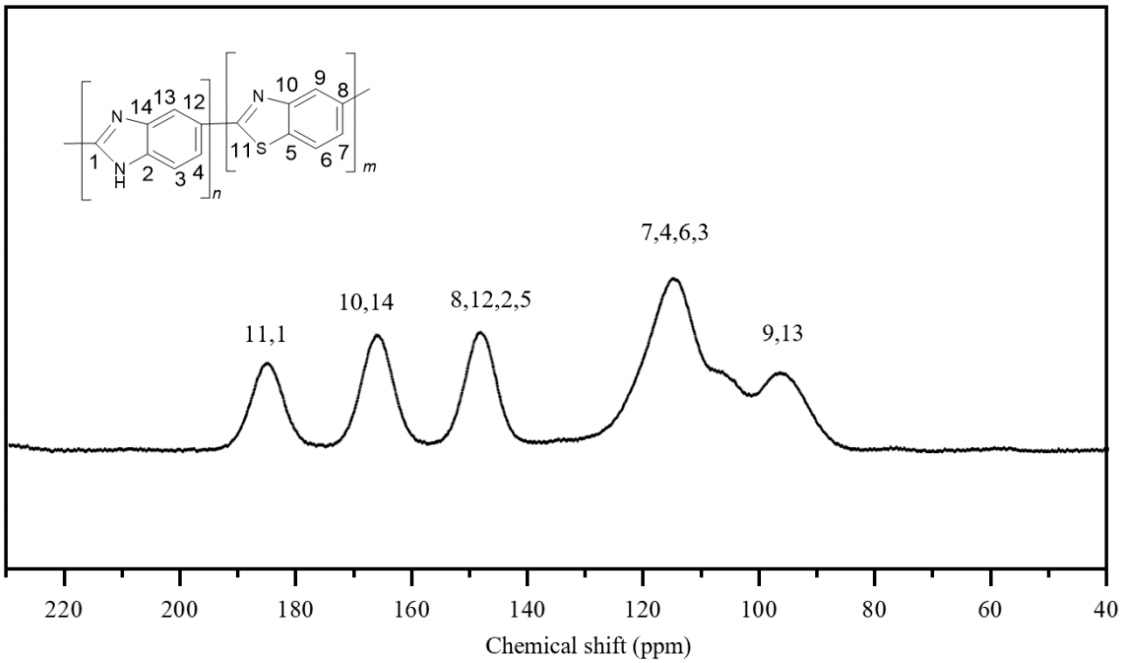

Figure 3.2. 13C solid-state NMR spectroscopy (CPTOSS) of PBT-*co*-PBI.

hetero rings and the carbon shared by hetero and benzene rings. The signal appears in about 167 ppm is attributed to the carbons in thiazole and imidazole hetero rings connected the nitro atoms. Finally, the one in about 188 ppm is attributed to the hetero atoms bonded with benzene rings.

3.3.2 Thermal properties

The thermal resistance is characterized by thermal gravimetric analysis (TGA). 5% and 10% weight loss temperature (T_{d5} and T_{d10}) are taken as indexes for the measurements. As is shown in **Figure 3.3,** T_{d5} and T_{d10} show regular changes with the changes of

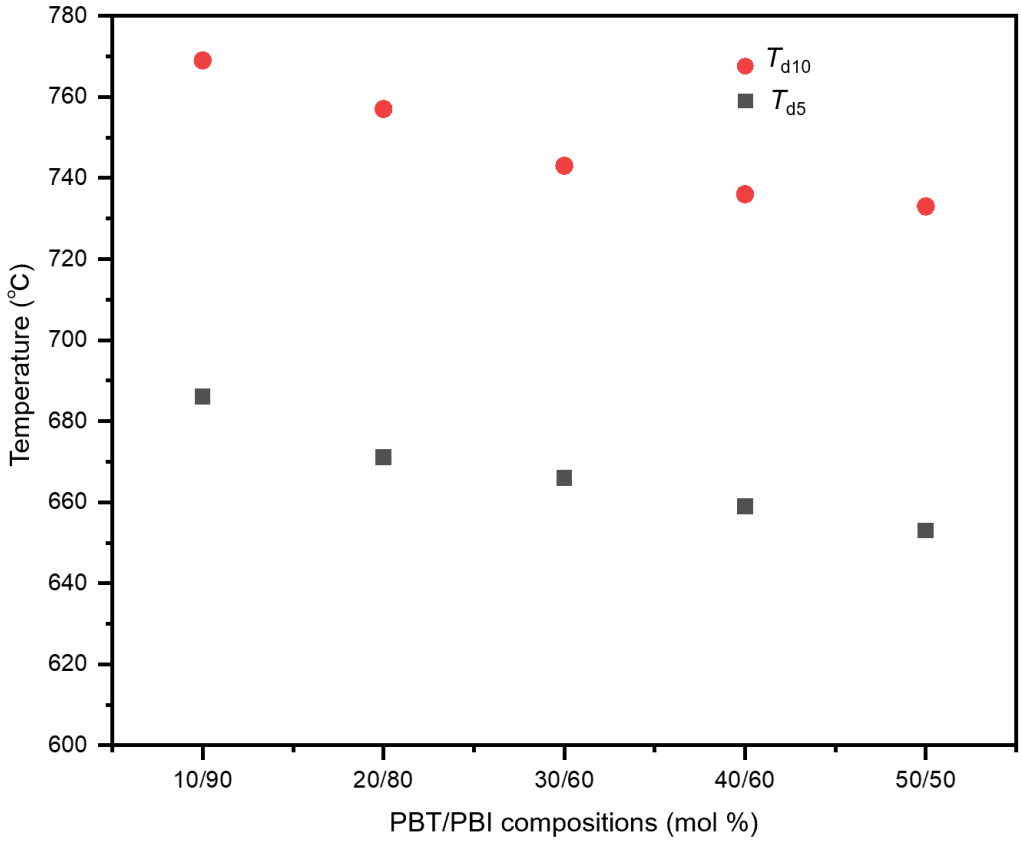

Figure 3.3. T_{d5} and T_{d10} of copolymer PBT-*co*-PBI.

polymer compositions. T_{d5} varies within the range of 653 ℃ to 686 ℃. the highest is shown by PBT-*co*-PBI of 90-10 mol% composition while the lowest temperature presented by 50-50 mol% compositions. T_{d5} increases with the increasing amount of PBI. T_{d10} presents the same trend with T_{d5}. T_{d10} changes within the temperature range of 733 to 769 ℃, the highest is shown by the copolymer with the composition of 90-10 mol% and the lowest one shown in the composition of 50-50 mol%. Like T_{d5}, T_{d10} shows a trend that increases with the increasing amount of PBI. This is presumably due to the hydrogen bond of PBI brings positive influence on the thermal stability of copolymers. The thermoresistance is heavily influence by 2 factors, one is the hydrogen bonding brought by PBI, and another is the strong aromaticity of PBT thiazoles, the thermal stability linearly decreases with the deceasing amount of PBI, indicating that the hydrogen bonding is probably the dominating factor to the thermal stability.

3.3.3 Dielectric properties

The dielectric constant (k) of the synthesized PBI-*co*-PBT films was characterized, the result is shown in **Figure 3.4a**. After drying at 100 deg for 12 h, the k of PBI-*co*-PBT varies from 3.2 to 2.8, decreases as increasing the molar composition of PBT. PBI-*co*-PBT in 50-50 mol% composition presents the lowest k value, indicating the copolymer film in this composition has the highest dielectric performance, this is presumably due

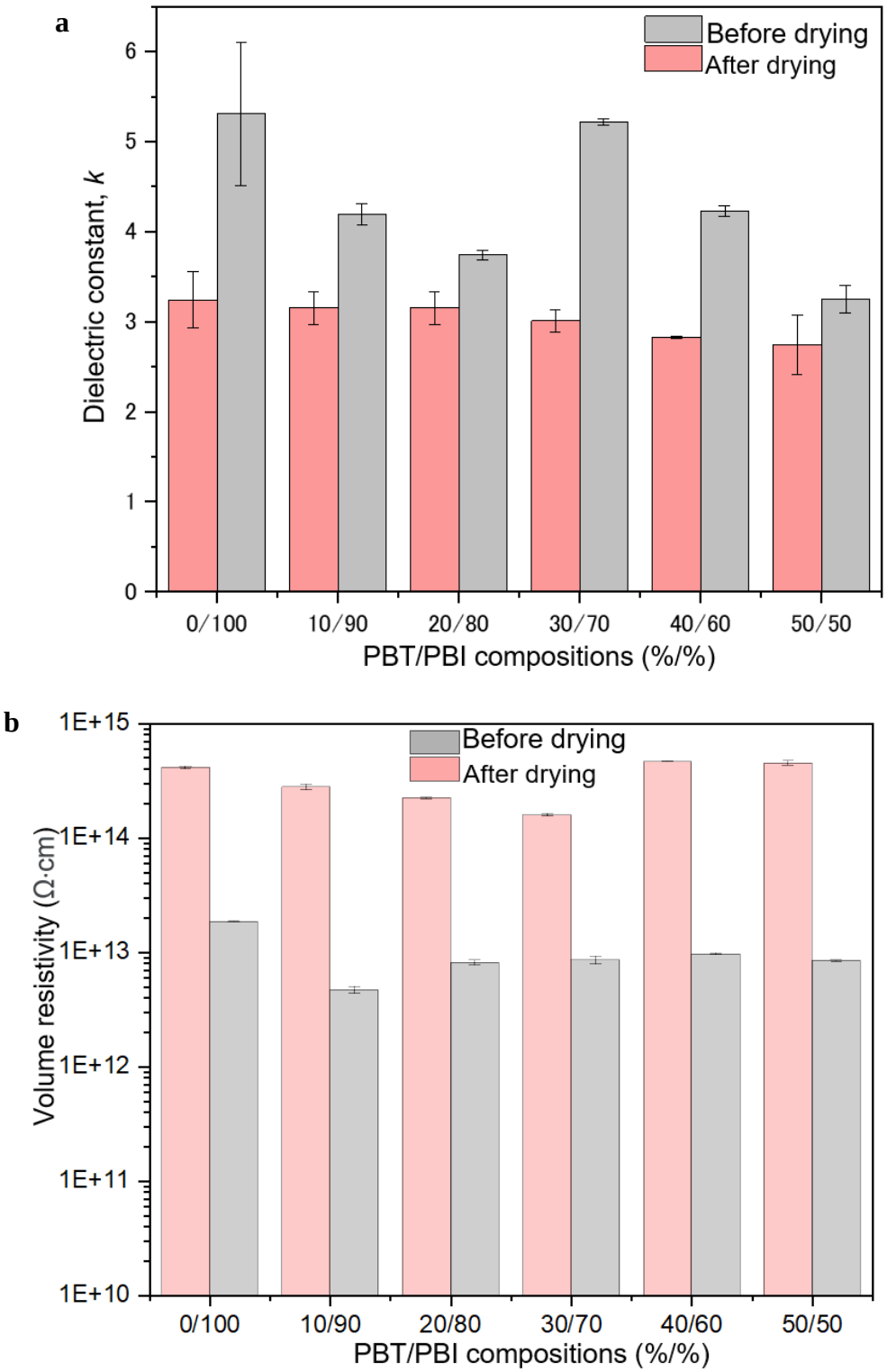

Figure 3.4. Dielectric constant (**a**) and volume resistivity (**b**)of PBT-co-PBI film in various compositions.

to the low polarizability of thiazoles of polybenzothiazoles, which is not as conductive

as imidazoles owing to the absence of proton in the thiazole rings. The k value increased to an extent when the film is not dying, this is due to the water effect of water absorbed in the films,

which probably increases the conductivity of film. Films in the entire molar compositions present a dielectric constant around 3, which is much lower than most of the commercially available polymer materials such as polyvinyl chloride (k = 4), indicating the copolymers can be utilized as great low-k material. High resistivity is shown in films of all compositions after drying, the values reach 10^{14} Ω·cm (**Figure 3.4b**), however, when water is absorbed, the resistivity decrease to approximately 10^{13} Ω·cm, indicating water brings the negative effect on film volume resistivity.

3.3.4 Mechanical properties.

PBT-*co*-PBT series of copolymers present low mechanical performance due to the high rigidity of polymer backbone. For example, PBT-co-PBI (20/80) shows a mechanical

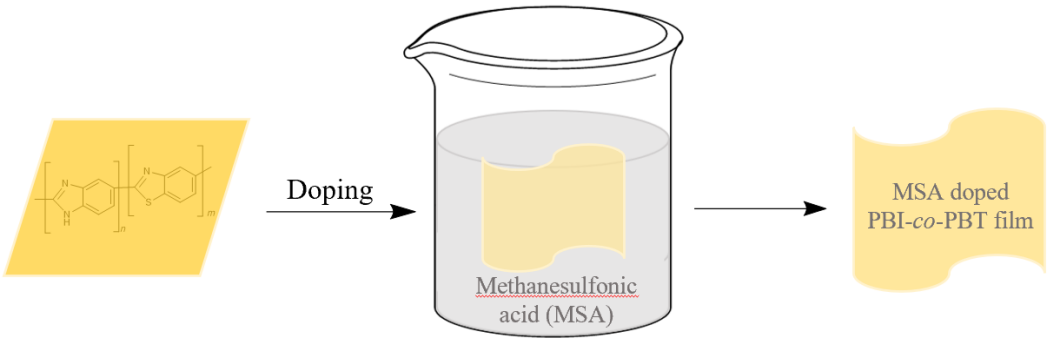

Figure 3.5. The illustration of film doping in MSA.

strength of 32 MPa and an elongation at break of 10%, suggesting the film is extremely brittle to utilized as a film in most application. In order to solve this problem, the film is doped by MSA to optimize the mechanical performance (**Figure 3.5**). As is shown in **Figure 3.6a,** after doping, mechanical strength decreased to 21 MPa while the fil m

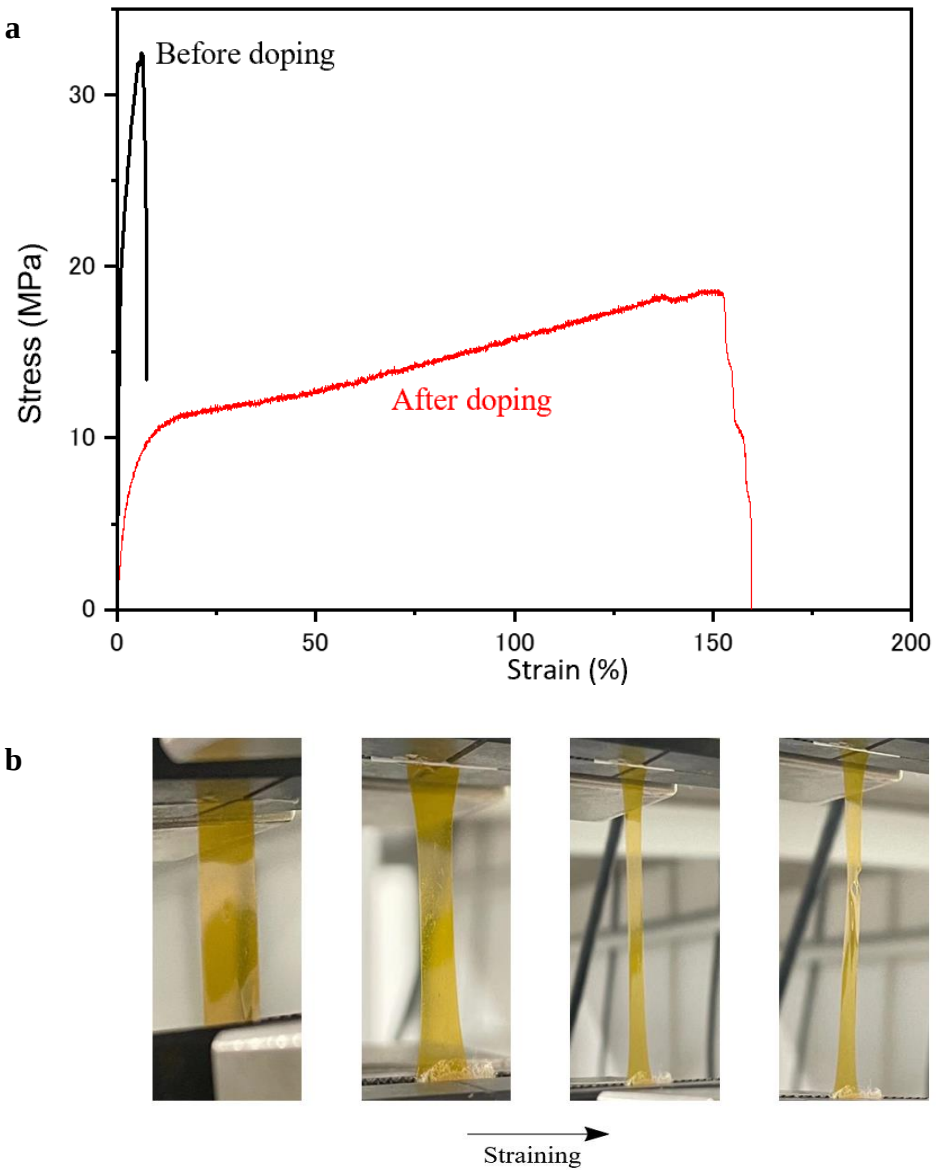

Figure 3.6. a. stress-strain curves of PBT-co-PBI film before and after doping by MSA; **b.** the images of straining film.

presents an elongation at break of 151%, approximately 15 times the value of pristine film. The film sample under stress-strain measurement is shown in **Figure 3.6b**, the film is extremely pliable under strain, indicating the mechanical optimization is successful. f

3.4 Conclusion

AMBA is synthesized from bio-derived monomer PABA, and the structure is confirmed by NMA. PBT-co-PBI series of copolymers are successfully synthesized via the copolymerization of AMBA and DABA, the obtained film showed an ultrahigh thermal stability, thermal decomposition temperatures decrease when increase the ratios of PBT, the highest 10% weight loss temperature reaches 760 degrees, higher than most organic materials, even comparable with some inorganic materials. Copolymer films in all compositions present high dielectric performance with dielectric constant around 3 and volume resistivity higher than $10^{14}\,\Omega\cdot$cm in dry state. The elongation of films can be optimized via doping experiment. The elongation at break of film in 20/80 mol% composition reaches 150%, indicating the copolymer can be used as high performance thermostable insulating films.

3.5 References:

1 M. G. A. Vieira, M. A. Da Silva, L. O. Dos Santos and M. M. Beppu, *Eur. Polym. J.*, 2011, 47, 254–263.

2 A. L. Andrady, *Mar. Pollut. Bull.*, 2017, **119**, 12–22.

3 Hisham A. Maddah, *Am. J. Polym. Sci.*, 2016, **6**, 1–11.

4 M. Khutia, G. M. Joshi, K. Deshmukh and M. Pandey, *Polym. Plast. Technol. Eng.*, 2015, **54**, 383–389.

5 T. Tanaka, G. C. Montanari and R. Mulhaupt, *IEEE Trans. Dielectr. Electr. Insul.*, 2004, **11**, 763–784.

6 Z. Deng, Y. Jiang, K. Chen, F. Gao and X. Liu, *Front. Microbiol.*, 2020, **11**, 353.

7 F. Leriche and J.-M. Zuliani, *Géographie, économie, société*, 2007, **9**, 19–38.

8 S. Becarelli, G. Siracusa, I. Chicca, G. Bernabei and S. Di Gregorio, *Water*, 2021, **13**, 3040.

9 Z. Liu, K. Wang, Y. Chen, T. Tan and J. Nielsen, *Nat. Catal.*, 2020, **3**, 274–288.

10 R. P. Babu, K. O'Connor and R. Seeram, *Prog. Biomater.*, 2013, **2**, 8.

11 J. Hildebrandt, A. Bezama and D. Thrän, *Waste Manag. Res. J. a Sustain. Circ. Econ.*, 2017, **35**, 367–378.

12 T. Garrison, A. Murawski and R. Quirino, *Polymers (Basel).*, 2016, **8**, 262.

13 A. Nag, M. A. Ali, M. Watanabe, M. Singh, K. Amornwachirabodee, S. Kato, T. Mitsumata, K. Takada and T. Kaneko, *Data Br.*, 2019, **25**, 104114.

14 T. P. Dawin, Z. Ahmadi and F. A. Taromi, *Prog. Org. Coatings*, 2018, **119**, 23–30.

15 J. Rajesh Banu, S. Kavitha, R. Yukesh Kannah, T. Poornima Devi, M. Gunasekaran, S.-H. Kim and G. Kumar, *Bioresour. Technol.*, 2019, **290**, 121790.

16 Z. N. Diyana, R. Jumaidin, M. Z. Selamat, I. Ghazali, N. Julmohammad, N. Huda and R. A. Ilyas, *Polymers (Basel).*, 2021, **13**, 1396.

Chapter IV

Design of biopolybenzazole exhibiting low dielectric constant and ultrahigh thermoresistance

Chapter IV

4.1 Introduction

Bio-based polymer materials developed from natural resources are sustainable and reliable, and therefore an ideal alternative to petroleum-based polymer materials.[1–5] Bio-based materials, such as poly(lactic acid) (PLA) and polyhydroxybutyrates (PHB), have been developed and used for various applications.[3,6,7] However, as most bio-based polymer materials have low thermal resistances and poor electric functions, they cannot be applied as engineering plastics that need to function in extreme conditions, such as in aerospace and electric vehicles, and high-power engines.[8–10]

Bio-based polybenzimidazole (PBI), which exhibits excellent thermal resistance, has been previously synthesized from 3,4-diaminobenzoic acid (DABA) *via* the Smiles rearrangement of the hydroxyl group of fermented 3-amino-4-hydroxybenzoic acid (AHBA).[11,12] In addition, poly(benzimidazole-*co*-amide) (PBI-*co*-PA) was synthesized by introducing amide groups to increase the processability of the polymer. Interestingly, it was found that the thermal decomposition temperature of PBI-*co*-PA increased with the incorporation of a small amount of PA (up to 15 mol%), in spite of the low degradation temperature of the PA units. Another PBI copolymer, poly(benzimidazole-*co*-benzoxazole) (PBI-*co*-PBO) was synthesized through the copolymerization of

DABA with AHBA. This copolymer exhibited excellent low dielectric constant (low-*k*) performance; however, its thermal stability and processability were not optimized.[13] Therefore, the development of a PBI derivative as a processable polymer material with outstanding thermal resistance and low-*k* performance remains a significant challenge.[9,14–16]

In this work, we design a series of PBI derivatives possessing improved thermal, mechanical and dielectric properties, by incorporating aramid and benzoxazole components into PBI. Among these derivatives, a terpolymer of appropriate composition exhibits a significant low *k*, as well as an ultrahigh thermodegradation temperature that is much higher than those of conventional polymers, including PBI and PBO.

4.2 Experimental section

4.2.1 Materials

AHBA (purity: > 97%), DABA (purity: 98%), 4-aminobenzoic acid (PABA) (purity: > 99%), and sodium hydroxide (NaOH) (purity: > 98%) were purchased from TCI (Tokyo Chemical Industry). Poly (phosphoric acid) (PPA) (purity: 85%) was obtained from Sigma-Aldrich. Methane sulfonic acid (MSA) (purity: > 98%) and trifluoroacetic acid (TFA) (purity: > 98%) were supplied by Wako pure chemical Industries, Ltd. pH test

paper, supplied by Macherey-Nagel GmbH & Co. KG, Düren, Germany). Copper wire were purchased from SENKO Co., Ltd. All the solvents and reagents in this research were used as received without any further processing or purification.

4.2.2 Syntheses

4.2.2.1 Monomers

DABA used in this work was synthesized from AHBA, which was obtained from nonedible cellulosic biomass. In the synthetic pathway, Smiles rearrangement was adopted to change the hydroxyl group into amine group, the specific synthesis information was reported in previous research.[13] DABA (6.0g, 31.5 mmol) was dispersed in 30 mL methanol and kept stirring. Hydrochloric acid (12 N) was added drop wise to the suspension until DABA was completely dissolved, after the color changed from pink to dark red, kept stirring at room temperature for 4 h. The pink salt of DABA dihydrochloride (DABA·2HCl) was obtained *via* solvent rotary-evaporation (yield: 5.4g, 94%). AHBA hydrochloride (AHBA·HCl) and PABA acid hydrochloride (PABA·HCl) salts were obtained following the same method as of DABA.

4.2.2.2 Simple terpolymerization

To synthesize the terpolymer, a simple polymerization reaction was performed, in which DABA·2HCl, AHBA·HCl, and PABA·HCl were simultaneously added to the reaction

system. The terpolymers were synthesized in PBI–PBO–PA compositions (mol%) of 70–30–0, 70–27–3, 70–21–9, 70–15–15, 70–9–21, 70–3–27 and 70–0–30, respectively. The synthesis of the terpolymer with a composition (mol%) of 70–21–9 is described below as a representative synthetic procedure. Herein, 25 g of PPA was taken in a three-necked round-bottomed flask with a magnetic stirrer and heated at 100 °C for 1 h in a nitrogen gas atmosphere to remove any traces of moisture. Subsequently, DABA ·HCl (940.8 mg, 4.20 mmol), AHBA·HCl (239.4 mg, 1.26 mmol), and PABA·HCl (93.9 mg, 0.54 mmol) were added to the flask, and the contents were stirred continuously for 1 h until all the moisture was eliminated, and the monomeric solids were completely dissolved in the reaction system. The mixture was then successively heated at 160 °C, 180 °C, and 200 °C for 4 h each, and ultimately at 220 °C for 12 h, during which the color of the solution changed from red to dark brown. The resultant solution was dispersed in water and stirred for 12 h to remove PPA; subsequently, a brown solid was obtained on filtration. After drying under vacuum, the solid was ground into a powder and suspended in deionized water. Then, 1M NaOH was slowly added, and the solution was stirred until the pH of the solution reached 7.0, and it was maintained for 1 h. The solid was collected by filtration and dried under vacuum to obtain a brown powder

(601.0 mg, 5.16 mmol) as the final product with a yield of 86%. An analogous synthetic process was performed for each of the terpolymers with other molar ratios.

4.2.2.3 Stepwise terpolymerization

Terpolymers were also synthesized using another method. The terpolymers were synthesized having the same BI-BO-A molar compositions with the simple terpolymerization. The terpolymer in composition of 70–21–9 (mol%) is described below as a representative synthetic procedure. Pre-polymerization of DABA was performed to prepare the polybenzimidazole homopolymer at the first synthetic step of the terpolymer, poly(benzimidazole-*block*-benzoxazole-*random*-aramid) (P(BI-*b*-BO-A)). Further, 25 g of PPA was taken in a three-necked round-bottomed flask with a magnetic stirrer, and heated at 100 °C for 1h in a nitrogen gas atmosphere to remove any traces of moisture. Then, DABA ·HCl (940.8 mg, 4.2 mmol) was slowly added to PPA, and the suspension was stirred for 1h. The temperature was then raised to 180 °C, and stirring was continued for another 1h to increase the viscosity, which indicated the polymerization of DABA to some extent.[16] Subsequently, the reaction system was cooled to 100 °C, and AHBA·HCl (239.4 mg, 1.26 mmol), and PABA·HCl (93.9 mg, 0.54 mmol) were added to the flask. The contents were stirred continuously for 1 h until all the moisture was removed and the monomeric solids were completely dissolved in

the reaction system. The mixture was then heated successively at 160 °C, 180 °C, and 200 °C for 4 h each and ultimately at 220 °C for 12 h, during which the color of the solution changed from red to dark brown. The resulting liquid was poured into water and stirred for 12 h to remove PPA; subsequently, a brown solid was obtained on filtration. After drying under vacuum, the solid was ground into a powder and suspended in deionized water. Subsequently, 1M NaOH (10%) was slowly added with stirring until the pH of the solution reached 7.0; it was maintained for 1 h. The solid was collected by filtration and dried under vacuum, and a brown powder (643.0 mg, 5.52 mmol) was obtained as the final product, with a yield of 92%. An analogous synthetic process was performed for each of the terpolymers with other molar ratios.

4.2.3 Measurements

Fourier transform infrared (FT-IR) spectra of terpolymers were recorded in a Perkin-Elmer Spectrum with a diamond-attenuated total reflection (ATR) accessory. The wavenumber range was set as 4000 to 400 cm^{-1}. Solid-state ^{13}C NMR CP/TOSS (Total Suppression of Spinning Sidebands) spectra of the terpolymer were recorded with a Bruker Advance III spectrometer operating at 500 MHz. Terpolymer samples were filled into 7 mm diameter zirconia rotor with a Kel-F cap and then spun at 8 kHz. The contact time and the period between successive accumulations were set as 2 s and 5s

respectively. The total number of the scans was set as 25000.

The viscosity of terpolymer was measured through a viscometer SIBATA 026300-3. Conc. sulfuric acid (H_2SO_4) was used as a solvent. Thermo-gravimetric analysis (TGA) curves of the terpolymers were recorded using a HITACHI STA7200. In a platinum crucible, the samples (5mg) were placed and heated under a nitrogen atmosphere to 1000 °C with a heating rate of 10 °C/min. The 5% mass loss temperature (T_{d5}) and 10% mass loss temperature (T_{d10}) of the samples were taken as indices of the thermal decomposition temperatures.

The stress-stain curves of the terpolymers were recorded *via* tensile mode mechanical tests using an Instron-3365 mechanical tester instrument at room temperature. Samples were shaped into a rectangular film with a length of 40 mm, width of 7 mm and a thickness of 15 μm. The elongation speed was set as 0.4 mm/min.

The electrical resistivity of the terpolymer films was measured using a digital megohmmeter (DSM-8104 HIOKI) at 25 °C. External electromagnetic noise was shielded by a Faraday cage during the measurement. Through conductive rubber electrodes with a guard electrode, two terminal methods were adopted to apply 1kV DC electric voltage to the film which had dimensions of 40×40 mm. The

formula $\rho_v = (S/t) \times R_m$ was used to calculate the volume resistivity ρ_v (Ω cm), where *S* is the area of the electrode, *t* represents the thickness of the film.

The crystallinity was investigated using an X-ray diffractometer (SmartLab; Rigaku Corp., Akishima, Japan). Wide-angle X-ray diffraction (WAXD) patterns was checked from the facade of the film with a graphite-monochromatized Cu Kα radiation beam generated at 100 mA and 40 kV.

The measurement of dielectric constant of the terpolymer films were carried out in an LCR meter (HIOKI IM3536) at 20 °C with a frequency of 1 MHz. The measurement was carried out by two terminals method with an applied electric potential of 1.0 V. The film was sandwiched between two electrodes with a constant pressure of 86 kPa and the sample holder was set in a Faraday cage. The relative dielectric constant (k_r) was calculated via the formula of $k_r = Cd/k_0A$, where *C* is the capacitance, *d* is thickness of film, *A* is the cross-sectional area of film and k_0 is the dielectric constant in vacuum ($=8.854\times10^{-12}$ F/m).

The coating experiment was performed using the copper wire with a diameter of 0.6 mm. In **Figure 4.9a**, the assembled mini motor is powered by 2 batteries of 1.5 V. In **Figure 4.9c,** two copper wires coated with terpolymer were connected with a sample holder made of strainless-steel in a parallel circuit. An electrical potential of 10 .0 V was

applied to the circuit using a dc power supply (PWR200MH KIKUSUI). Both copper wires were approximately 8.0 cm long, therefore the electric current flowed could be same for both wires. The electric current flowed in the main circuit was measured to be 16.0 A.

4.2.4 Theoretical Calculations

To understand thermal stability of the terpolymer, we made several trimer models (**Table 4.2**) and evaluated their interaction enthalpies of the H-bonds between molecular chains theoretically, following our previous study:[13] All the DFT simulations were carried out using Gaussian 16.[18] To properly describe the charge transfer relevant to the H-bonds, CAM-B3LYP was chosen as the exchange-correlation functional,[19] associating with the cc-pVQZ basis set.[20] A basis-set superposition error was reduced by applying the counterpoise correction to optimize each of the geometries.[21]

Scheme 4.1. Synthetic pathway of terpolymers from three aminobenzoic acid derivatives through simple polymerization. Inset: picture of cast film.

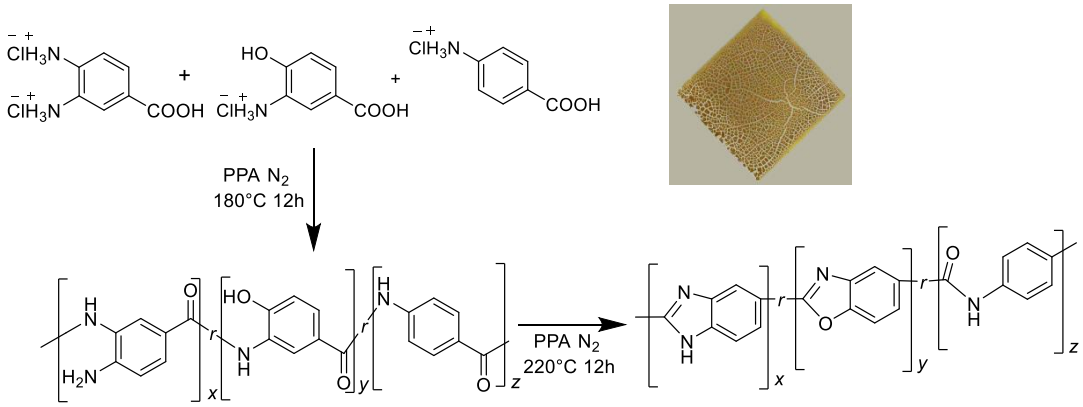

Scheme 4.2. Synthetic pathway of P(BI-*b*-BO-A) from three aminobenzoic acid derivatives through stepwise polymerization.

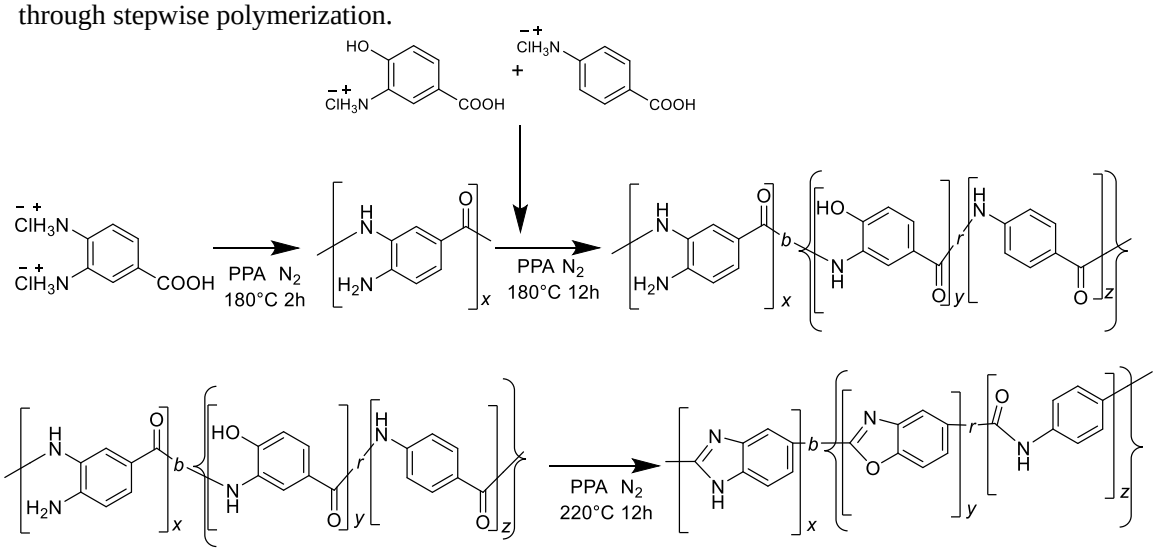

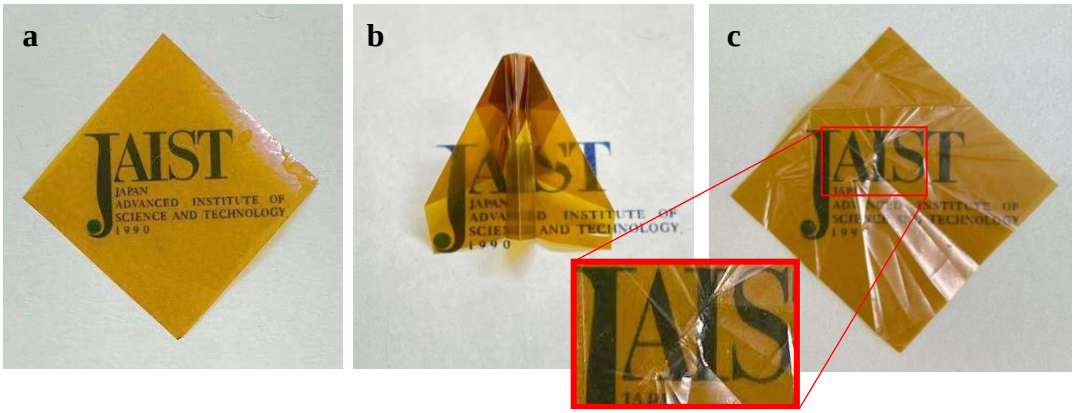

Figure 4.1. Images of the solution casted film of terpolymer. **a** Pristine, **b** origami-folded, and **c** unfolded films.

4.3 Results and discussions

4.3.1 Syntheses

At first, the terpolymers were synthesized in bulk by a simple polymerization method. Although the polymerization mixture became viscous and the reaction appeared successful, casting of the resulting polymers did not produce self-standing films, as can be seen from the photograph in the inset of **Scheme 4.1**. If the macromolecular backbone is too rigid, processing becomes difficult in some cases. Considering the good processability of PBI, as shown in previous reports,[9,13] it was hypothesized that the continuous structure of benzimidazole units might be effective for film preparation.

Therefore, a stepwise method was adopted for the synthesis; at first, the polybenzimidazoles were synthesized for short-range polymerization; then, the monomers for PBO and PA were added and successively polymerized to produce poly(BI-*b*-BO-A), as shown in **Scheme 4.2**. The cast of poly(BI-*b*-BO-A) (100.0 mg, 0.2 mmol) was made over TFA solution (3 mL) containing 2 drops of MSA on a silicon substrate. After drying at 25 °C, the film was scratched off the substrate and then immersed in deionized water for 12 h to remove the residual acid. The self-standing film was successfully fabricated, and the film was further dried at 80 °C for 12 h (**Figure 4.1a**). The film was pliable enough to be folded into the shape of an origami

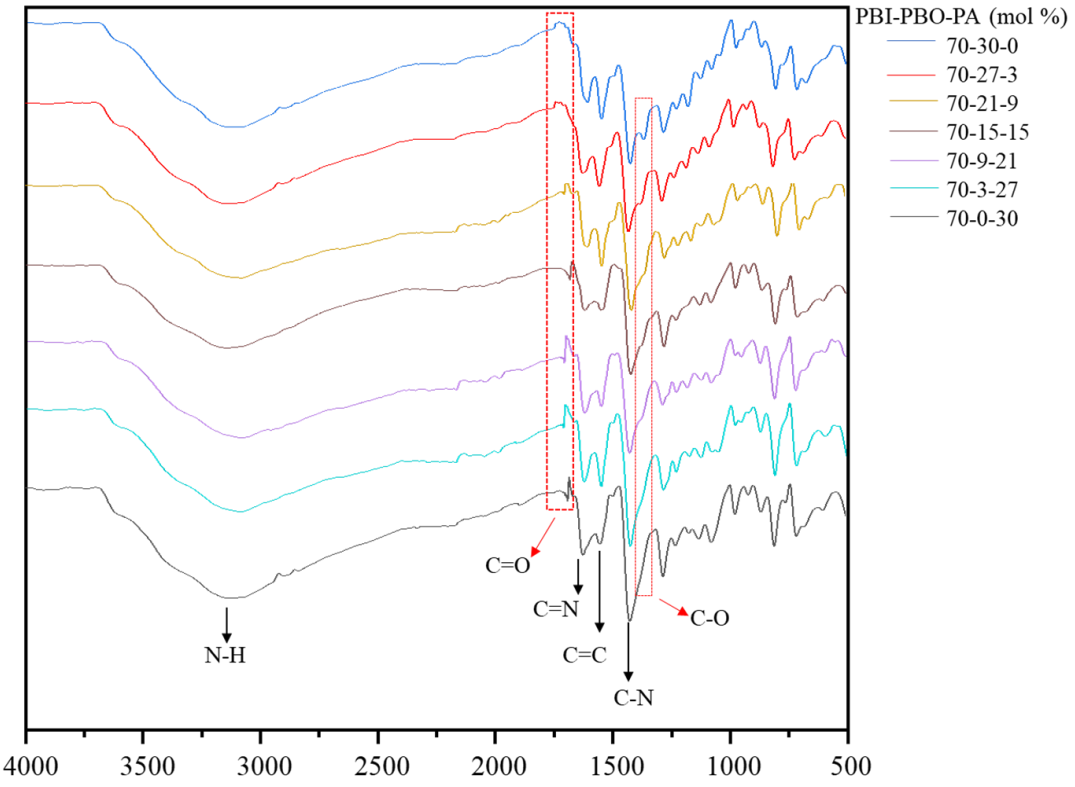

Figure 4.2. FT-IR spectra of terpolymer in various molar compositions.

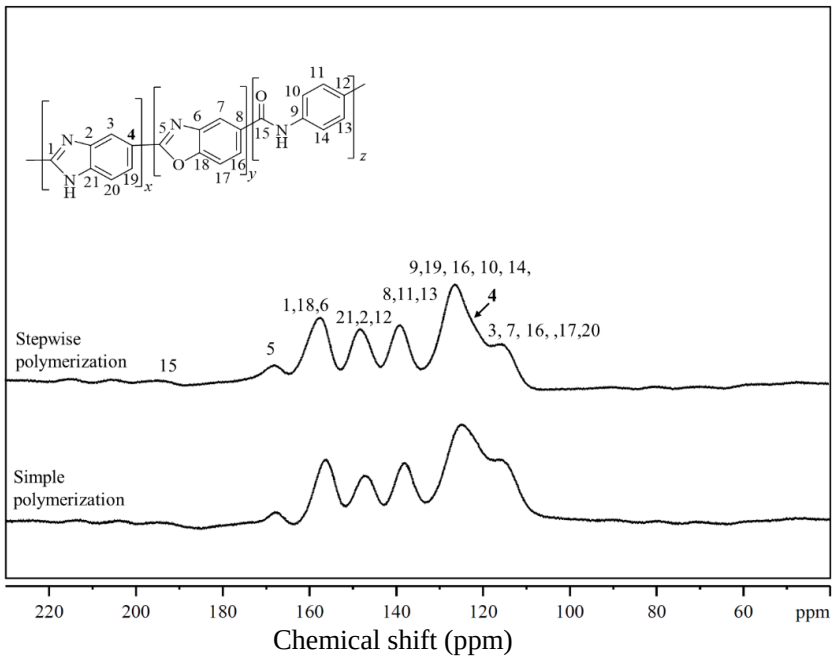

Figure 4.3. Solid-state ^{13}C CP/TOSS NMR spectra of terpolymers in 70–21–9 (mol%) prepared by a simple polymerization and a stepwise polymerization method.

airplane (**Figure 4.1b**); after unfolding, it did not tear or break (**Figure 4.1c**).

The structures of the polymers were confirmed by Fourier Transform-Infrared (FT-IR) and ^{13}C solid-state Nuclear Magnetic Resonance (NMR) spectroscopies. In the FT-IR spectra (**Figure 4.2**), for terpolymer in all the ratios, distinct C=N, C=C, and C-N absorption peaks were observed at approximately 1690 cm^{-1}, 1590 cm^{-1} and 1380 cm^{-1} respectively. Besides, the C=O absorption peaks gradually showed at approximately 1745 cm^{-1} and became stronger as PA ratio increasing from 0 to 30%, but the C-O peaks became weaker and vanished ultimately because of the decreasing composition of PBO. In the solid-state NMR spectrum (**Figure 4.3**), six distinct signals in the range of 100 to 180 ppm and some very broad signals between 190 and 220 ppm were detected. The signal at 167 ppm was assigned to oxazole carbon (marked as 5), and the signal at 160 ppm contained the imidazole carbon (marked as 1) among others. Very broad signals in the range of 190 to 220 ppm were assigned to amide carbonyl carbons that connect BI and BO to A. The other signals were assigned to the benzene carbons. The close resemblance between the solid-state NMR spectra of the polymers synthesized *via* simple and stepwise polymerization, suggested that they had analogous structures. The NMR signal from the carbon marked as 4 (C_4), is expected to be sensitive to the presence of neighboring units such as BI, BO, and A. Therefore, the broadness of this signal for the polymer prepared

by simple polymerization can be attributed to the presence of all the three neighboring units around C_4. In contrast, the sharper C_4 signal detected for the polymer prepared by stepwise polymerization can be explained by the PBI block formation.

The molecular weight of the polymers could not be evaluated by chromatography owing to their poor solubility in popular solvents. However, the inherent viscosities (η_{inh}) of the polymers were evaluated in a solution of concentrated sulfuric acid to compare their degrees of polymerization, as described in **Table 4.1.** The inherent viscosities of terpolymers synthesized by stepwise polymerization ($\eta_{inh\ 1}$) ranged from 1.24 to 1.89 dL/g, which are much higher than those of the terpolymers synthesized by simple polymerization (η_{inh2}: 0.64–0.84 dL/g). DABA possesses a high polymerizability owing to the reactive functional groups of *o*-diamine. The higher values of $\eta_{inh\ 1}$ compared to $\eta_{inh\ 2}$ are responsible for the formation of the pliable film from P(BI-*b*-BO-A) (**Figure 4.1**). In addition, η_{inh} decreases with a decrease in the amount of PBO (and increase in PA) for both types of terpolymers. This can be attributed to the higher amine reactivity due to the presence of *the o*-hydroxy groups.

Table 1. Thermal and mechanical properties of bio-based terpolymers.

Polymer composition[a] (%)	T_{d5}[b] (°C)	T_{d10}[b] (°C)	σ[c] (MPa)	γ[c] (%)	E[c] (GPa)	η_{inh1} (η_{inh2})[d] (dL/g)
70-30-0	638	703	80±1.5	2.3±0.1	3.48	1.89 (0.84)
70-27-3	634	701	76±3.2	3.2±0.2	2.38	1.75 (0.78)
70-21-9	624	707	76±1.0	5.1±0.1	1.49	1.65 (0.77)
70-15-15	637	716	74±1.4	6.7±0.1	1.23	1.38 (0.78)
70-9-21	658	736	72±1.2	8.6±0.1	0.84	1.30 (0.75)
70-3-27	675	758	63±1.7	10.3±0.1	0.61	1.28 (0.74)
70-0-30	686	763	48±1.6	12.0±0.2	0.40	1.24 (0.64)

a) Terpolymers in varying compositions of PBO and PA, in which PBO varied from 30% to 0 while PA composition varied from 0 to 30%. PBI composition were fixed at 70%. b) Thermal property indices, measured by TGA at nitrogen atmosphere. 5% and 10% weight loss thermal decomposition temperatures (T_{d5} and T_{d10}). c) Mechanical properties *σ, γ, and E* measured by stress-strain tensile test *refer to tensile strength at break, strain at beak, and Young's modulus, respectively*. d) η_{inh1} refers to inherent viscosity of terpolymer synthesized by stepwise polymerization, while η_{inh2} shown in parentheses refers to inherent viscosity of terpolymer synthesized via regular polymerization.

4.3.2 Thermal properties

The thermal stabilities of the terpolymers synthesized by stepwise polymerization were estimated using Thermogravimetric Analysis (TGA) under a nitrogen gas atmosphere. According to the thermograms obtained (**Figure 4.4a**), none of the terpolymers were found to exhibit any significant loss of mass up to ~520 °C; mass loss started occurring at approximately 550 °C. Significant mass losses were observed with an increase in temperatures up to 1000 °C. Interestingly, the completion of thermal degradation was not detected below 1000 °C, and the residue yields were still higher than 69 wt%. The thermal decomposition temperatures T_{d5} and T_{d10} for P(BI-*b*-BO-A) of all compositions

have been listed in **Table 4.1** and plotted against the PA compositions in **Figure 4.4b.** Both T_{d5} and T_{d10} were almost constant for low mole percentages of PA. However, beyond a critical PA composition of 9 mol%, they gradually increased with increasing mol% of PA. Terpolymers having 30 mol% of PA showed the highest T_{d5} and T_{d10} values of 686 °C and 763 °C, respectively. This can be attributed to the occurrence of inter-chain hydrogen bonds between the imidazoles and primary amines, which increase in number with the increase in relative mol% of PA compared to benzoxazoles. Overall, the terpolymers were found to exhibit ultrahigh thermal stability, and a T_{d10} of ~760 °C, which is the highest value reported so far for plastic films, and is comparable to the melting points of light metals such as aluminum and magnesium.

The burning characteristics of the terpolymers were investigated using a combustion test, in which a terpolymer film with a composition of 70%–21%–9% was taken as the representative terpolymer and a polyethylene film was used as the reference. Unlike that for the polyethylene film, no obvious flame was visible during the burning of the terpolymer film (**Figure 4.4c**). In addition, the ignition of the terpolymer film was quenched immediately after removal from the fire, and no dripping of the material was observed during the entire test, suggesting that the terpolymer film is extremely flame-retardant.

To elucidate the mechanism of thermal stability of the terpolymer, the interaction enthalpy of the hydrogen bonds (H-bonds) between its molecular chains was investigated *via* density functional theory (DFT) calculations. Several trimer models comprising three units of 2-phenylbenzimidazole (2BI), 2-phenylbenzoxazole (2BO), and benzanilide (BA) were used to simulate the polymer chains. Since PBI had the highest composition (70 mol%) in our terpolymers, the interaction enthalpy of the hydrogen bonding between imidazole N-H (model 1) and imidazole N (model 2) were calculated in detail. The results have been presented in **Table 4.2.** The interaction enthalpy for H-bonding between the two BI primary models was calculated to be −13.32 kcal/mol, which was higher than that calculated for any other combination of BI, BO and BA primary models (entries 1-5). The results indicate that the H-bonding between two imidazole rings is the strongest of the five combinations. Next, the models were extended to trimers with BI as the central unit. In a previous work from our group, the H-bonding between two models of BI-BI-BI was found to be very weak (with an interaction enthalpy of −4.77 kcal/mol), presumably due to the lowered reactivity of both N-H and -N= by resonance stabilization in the long π-conjugation (entry 6).[13] However, the incorporation of BA in either one of the two trimer models was found to increase the H-bond interaction enthalpies (entries 7-10). In the present study, it was

observed that the H-bonding was strengthened by the incorporation of BO and BA on both sides of the central BI. The interaction enthalpy between the two trimer models of BA-BI-BA (entry 11) was estimated to be −14.13 kcal/mol, which is slightly higher than that of entry 1, owing to the limitation of resonance stabilization, and the possible induction effects due to the substitution with BA. For BO-BI-BO and BO-BI-BA, the H-bonding enthalpies were calculated to be −13.57 kcal/mol and −13.80 kcal/mol, respectively. The absolute values of the H-bonding interaction enthalpies were found to increase with increase in the amount of incorporated PA, indicating an elevation in the interaction enthalpy of the H-bond due to the incorporation of PA into PBI chain, thereby increasing the thermal stability.

Table 4.2. Interaction enthalpy values of H-bond in various models.

entry	Monomer1 (H-donor)	Monomer2 (H-acceptor)	Interaction enthalpy (kcal/mol)
1 [b]	BI	BI	-13.32
2 [b]	BI	BO	-9.23
3 [b]	BI	BA	-10.24
4 [b]	BA	BO	-9.23
5 [b]	BA	BA	-6.85
6 [a]	BI-BI-BI	BI-BI-BI	-4.77
7 [a]	BA-BI-BI	BI-BI-BI	-10.58
8 [a]	BI-BI-BI	BA-BI-BI	-10.01
9 [a]	BI-BI-BA	BI-BI-BI	-12.46
10 [a]	BI-BI-BI	BI-BI-BA	-12.68
11 [b]	BA-BI-BA	BA-BI-BA	-14.13
12 [b]	BO-BI-BO	BO-BI-BO	-13.57
13 [b]	BO-BI-BA	BO-BI-BA	-13.80

a)H-bonding enthalpy calculated via DFT theory. b) H-bonding enthalpy calculated via DFT theory in previous work.

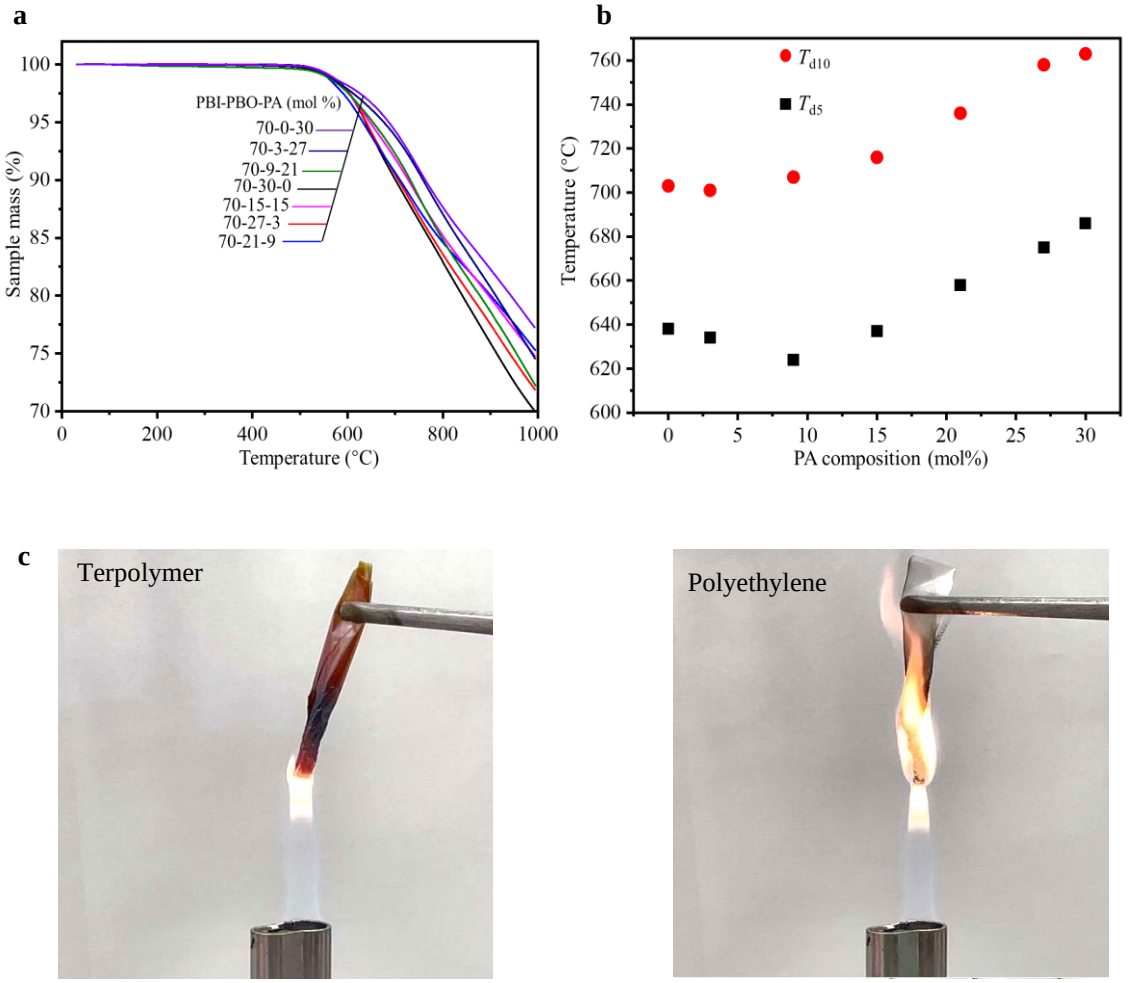

Figure 4.4. Thermal characterization of terpolymers. **a** TGA curves of terpolymers with various compositions. **b** T_{d5} and T_{d10} of terpolymers of different compositions. **c** Burning photographs depicting the burning terpolymer (left) and polyethylene (right).

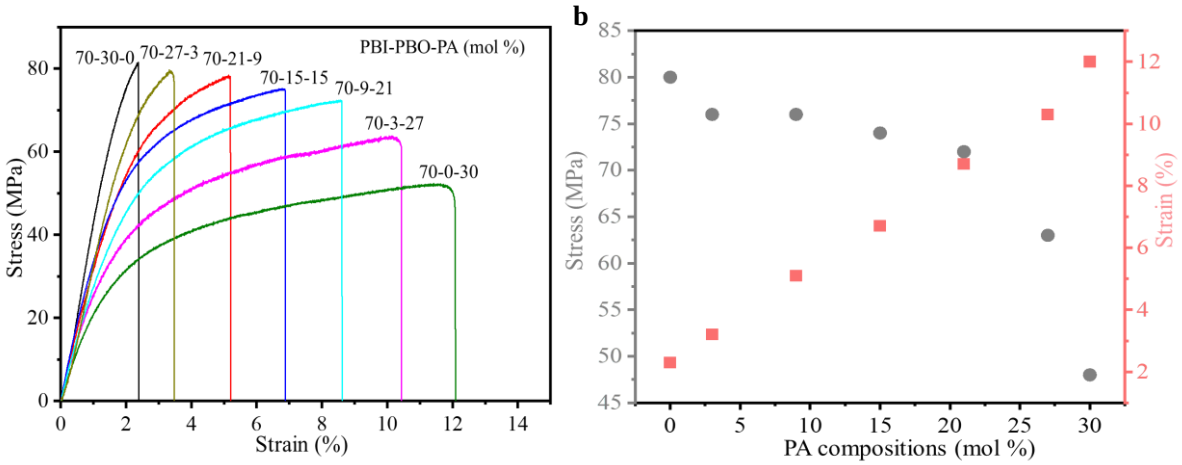

Figure 4.5. Mechanical properties of terpolymers. **a** Stress-strain curves of terpolymers. **b** Tensile stress and strain values in different PA compositions.

4.3.3 Mechanical properties

The mechanical properties of the terpolymer films synthesized by stepwise polymerization were investigated using the stress–strain analysis (**Figure 4.5a**). The tensile strength at break (σ), strain at break (ε), and Young's modulus (E) were evaluated therefrom. The stress–strain curves showed a consistent increase of stress with strain up until the breakage point, corresponding to the maximum permissible strain (strain at break or ε, **Table 4.1**). The values of the mechanical properties showed regular variations with the molar compositions of PA (**Figure 4.5b**). With the increase in mole% of PA, the value of strain at break increased from 2.3% to 12.0%, while the tensile strength decreased from 80 MPa to 48 MPa, and the Young's modulus decreased from 3.48 GPa to 0.40 GPa. The terpolymers with higher mol% of PA exhibited higher ε and lower E values, presumably due to their greater abundance of non-heterocyclic PA components that are expected to be more flexible than the heterocyclic PBO components.

4.3.4. Dielectric properties

Dielectric measurements were performed using the films obtained from P(BI-*b*-BO-A) synthesized by stepwise polymerization. The thicknesses of the terpolymer films were maintained between 7.0 to 10.0 μm for the dielectric measurements. The values of the

different parameters obtained from these measurements, for the terpolymer films of different compositions, have been listed in **Table 4.3**. **Figure 4.6a** shows the volume resistivity for dried P(BI-*b*-BO-A) films as a function of PA composition. The volume resistivity for terpolymer with a PA mole composition (r_{PA}) of 3 % was equal to that for P(BI-*b*-BO) (r_{PA}=0) at approximately 6.22×10^{11} Ωcm and it significantly increased to 1.24×10^{14} Ωcm at r_{PA}=9%, suggesting that the terpolymer changed to highly insulative. However, it suddenly decreased to 2.67×10^{10} Ωcm at r_{PA}=15%, showing that the terpolymer transforms to a low insulator where the resistivity is more than an order of magnitude lower than that of P(BI-*b*-BO) (r_{PA}=0). At a region above 15%, the volume resistivity was independent of the PA composition. This drastic change in volume resistivity in the vicinity of r_{PA}=10% is considered to be a structural transition with nano- or submicron- scale although there was no remarkable change in the appearance or transparency of the films. The structural transition was confirmed through X-ray diffraction shown in **Figure 4.7**. In electrically heterogeneous materials, even if morphologically uniform, the bulk electrical resistivity is strongly dominated by the local resistivity. Therefore, it can be considered that the low resistivity at r_{PA}>15% was caused by the occurrence of a continuous phase with low resistivity having a wide distribution of resistance in a highly insulative matrix.[22,23] On the contrary, it can be

considered that the significant increase in the resistivity at r_{PA}<9% is due to an electrically homogeneous and high resistivity phase rapidly develops in the whole bulk of terpolymer by incorporating PA and reducing PBO. Thus, in order to understand the complex behavior of the volume resistivity, it is necessary to consider the electrical homogeneity of the resulting terpolymers.

Figure 4.6b shows the relative dielectric constant at 1 MHz for dried P(BI-*b*-BO-A) films as a function of PA ratio. The dielectric constant seems to have increased monotonously with the PA ratio although there was some variation. PBO units have a rigid aromatic backbone, resulting in a low mobility of charge in response to electric field, and the lower polarizability of the oxazoles contributed to the lower dielectric constant values for the terpolymers with higher mol% of PBO (and lower mol% of PA). It is shown below that the dielectric constant has to be considered for electrical uniformity in the same way as the resistivity. The observed dielectric constant k_{obs} for a dielectric substance consisting of several components with different dielectric property can be explained as the following equation when a parallel connection of capacitances is hypothesized,

$$\frac{1}{k_{obs}} = \sum_n \frac{\varphi_n}{k_n} \quad (1)$$

, where k_n and φ_n represent the relative dielectric constant and the fraction of each component. For the terpolymer system studied here, the observed dielectric constant k_{obs} can be explained as,

$$\frac{1}{k_{obs}} = \frac{\varphi_{PBI}}{k_{PBI}} + \frac{(1-\varphi_{PBI})(1-r_{PA})}{k_{PBO}} + \frac{(1-\varphi_{PBI})r_{PA}}{k_{PA}} \quad (2)$$

, where k_{PBI}, k_{PBO}, k_{PA} are the relative dielectric constant for neat PBI, PBO, and PA. ϕ_{PBI} is the volume fraction of PBI, and r_{PA} stands for the PA ratio. The experimental data was fitted by eq. (2) using a synthesis condition of φ_{PBI} =0.7 and a measured value of k_{PBI} =3.4. The result of fitting is represented as the broken red line in **Figure 4.6b** and showed that the dielectric constant for PBO and PA was calculated to be 2.0 and 1.3, respectively. The dielectric constant for a neat PBO film after drying was measured to be 1.9, which was close to the value obtained by the fitting. However, the value of dielectric constant for PA is extremely low. Therefore, it is clearly that the observed dielectric constant cannot be explained by the parallel model of capacitors in eq. (2). The degree of crystallinity was clearly dropped off at 9%<φ_{PA}<15% (**Figure 4.7**), therefore, it was considered that the dielectric property is strongly affected by a

structural transition in local similarly to the volume resistivity.

Figure 4.8 shows a plot of the dielectric constant versus 1% thermal degradation temperature (T_{d1}) of the obtained terpolymers alongside other commercially available polymer materials. Generally, polymer materials with low dielectric constants show relatively low thermal resistance, while those with higher dielectric constants exhibit higher thermal resistance. For example, polypropylene (PP), polystyrene (PS), and poly(butyl methacrylate) (PBMA) which have low dielectric constant values (2.2, 2.6, and 2.7 respectively), also have low T_{d1} values (310, 375, and 350 °C respectively).[24-29] In contrast, polymers like polyphenylene sulfide (PPS), polyimide (Kapton^{TM}), and polyether ether ketone (PEEK), which exhibit high thermal resistance with high T_{d1} values (495, 500, and 525 °C respectively), also have relatively high dielectric constant values (3.8, 3.3, and 3.4, respectively)[30-35]. Compared to the aforementioned polymers, Zylon exhibits a relatively low dielectric constant and a high thermal resistance, presumably due to the effects of its benzoxazole structure.[36,37] The lowest dielectric constant among the terpolymers synthesized in the present work was found to be 2.4, which is extremely low compared to that of different commercially available polymer materials. Considering its outstanding thermal resistance, we can conclude that this terpolymer exhibits the best performance among all the polymers that have been

compared. Overall, the P(BI-*b*-BO-A) films can be considered reliable as thermoresistant insulators that can withstand ultrahigh operating voltages.

Table 4.3. Dielectric property indices of the terpolymers having various compositions.

Polymers (PBI-PBO-PA %)	d [a] (μm)	k_r [b]	ρ_v [c] (Ω · cm)
70-30-0	7.0	2.6	6.22E+11
70-27-3	8.0	2.4	6.63E+11
70-21-9	10.0	3.0	1.24E+14
70-15-15	6.0	2.6	2.67E+09
70-9-21	7.0	2.8	3.67E+10
70-3-27	8.0	2.9	5.12E+10
70-0-30	9.0	3.2	4.09E+10

a) Thickness b) Dielectric constant; c) Volume resistivity.

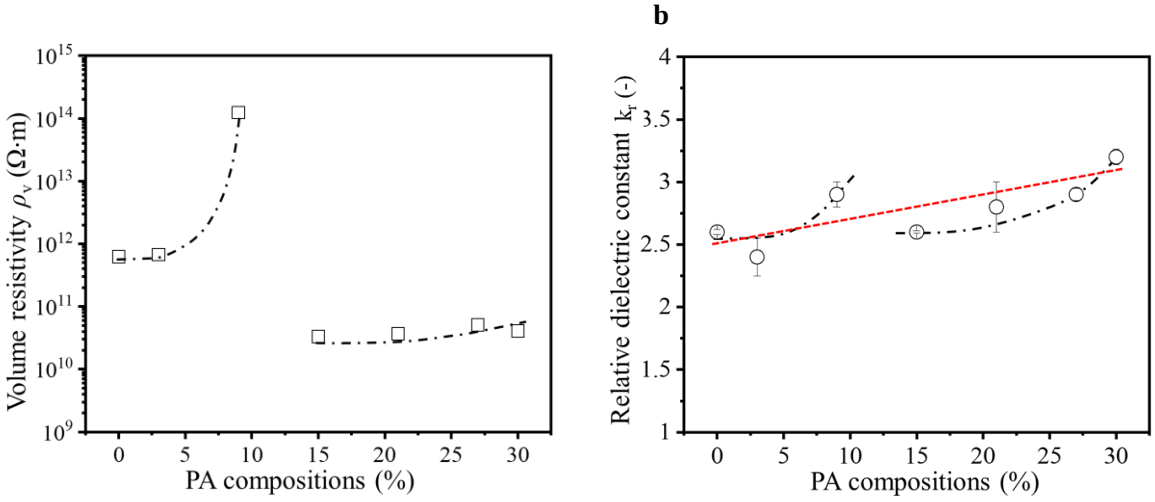

Figure 4.6 Dielectric properties of terpolymers. **a** Volume resistivity and **b** relative dielectric constant at 1 MHz for dried P(BI-*b*-BO-A) films of different PA compositions. The broken lines were drawn by naked eyes and the dotted line in **b** was drawn by eq. (2)

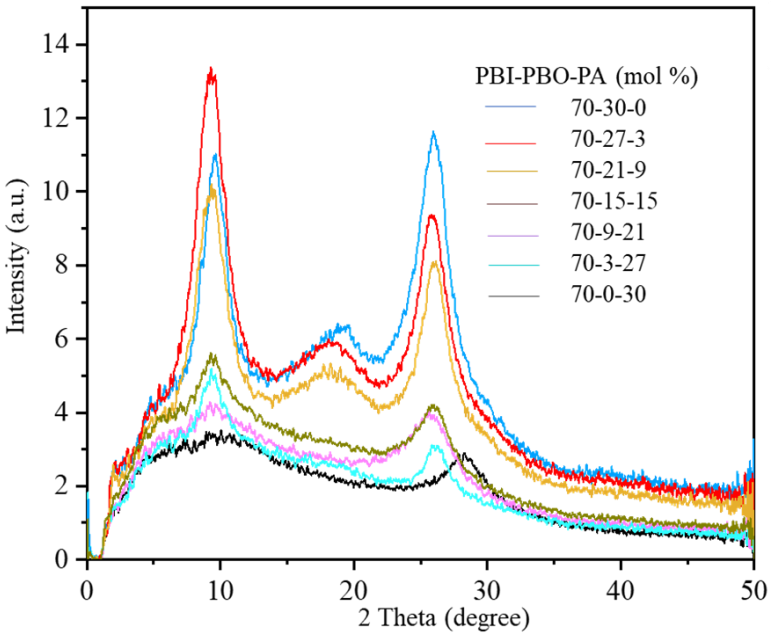

Figure 4.7. XRD spectra of terpolymer films

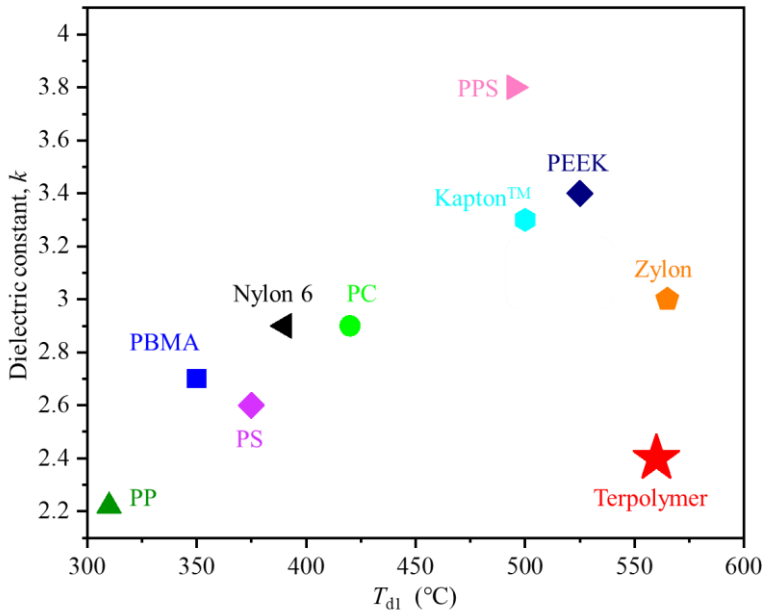

Figure 4.8. Plot of diele ctric constant versus 1% thermal degradation temperature (T_{d1}) for the terpolymer and other common commercial polymer materials.

4.3.5 Coating

A coating experiment was conducted to investigate the applicability of the obtained P(BI-*b*-BO-A) as an insulator. For this, a solution of P(BI-*b*-BO-A) (mol% composition of 70-15-15) in TFA (70 mg/3mL) was prepared, and a spiral coil of copper wire was soaked in it for 2 mins. On removing from the solution and drying in air, a thin layer of the polymer was coated onto the surface of the copper wire (**Figure 4.9a**). To investigate its dielectric performance, the coil of copper wire coated with P(BI-*b*-BO-A) was equipped with a magnet to assemble a mini motor model (**Figure 4.9b**). The coil rotated successfully after being powered on, indicating that the coating layer functioned as an insulator. In addition, the thermal resistance of the P(BI-*b*-BO-A)-coated copper wire was compared with commercial copper wire (polyurethane enameled copper wire) by simultaneously applying a direct current (16 A, 10 V). Since the electric circuit is parallel and the length of the copper wires is same, the electric current and the resultant Joule heat should be the same for both samples. When the current was gradually increased, the commercial copper wire started giving off smoke while the P(BI-*b*-BO-A)-coated one remained stable (**Figure 4.9c**). Both coils were observed using SEM to check the condition of their surfaces after the experiment. The coating layer of the commercial copper wire presented a significant amount of damage (**Figure 4.9d**), whereas no significant damage was observed in the P(BI-*b*-BO-A) coating layer

(**Figure 4.9e**). Thus, we can confirm that P(BI-*b*-BO-A) works as a thermostable insulating coating material.

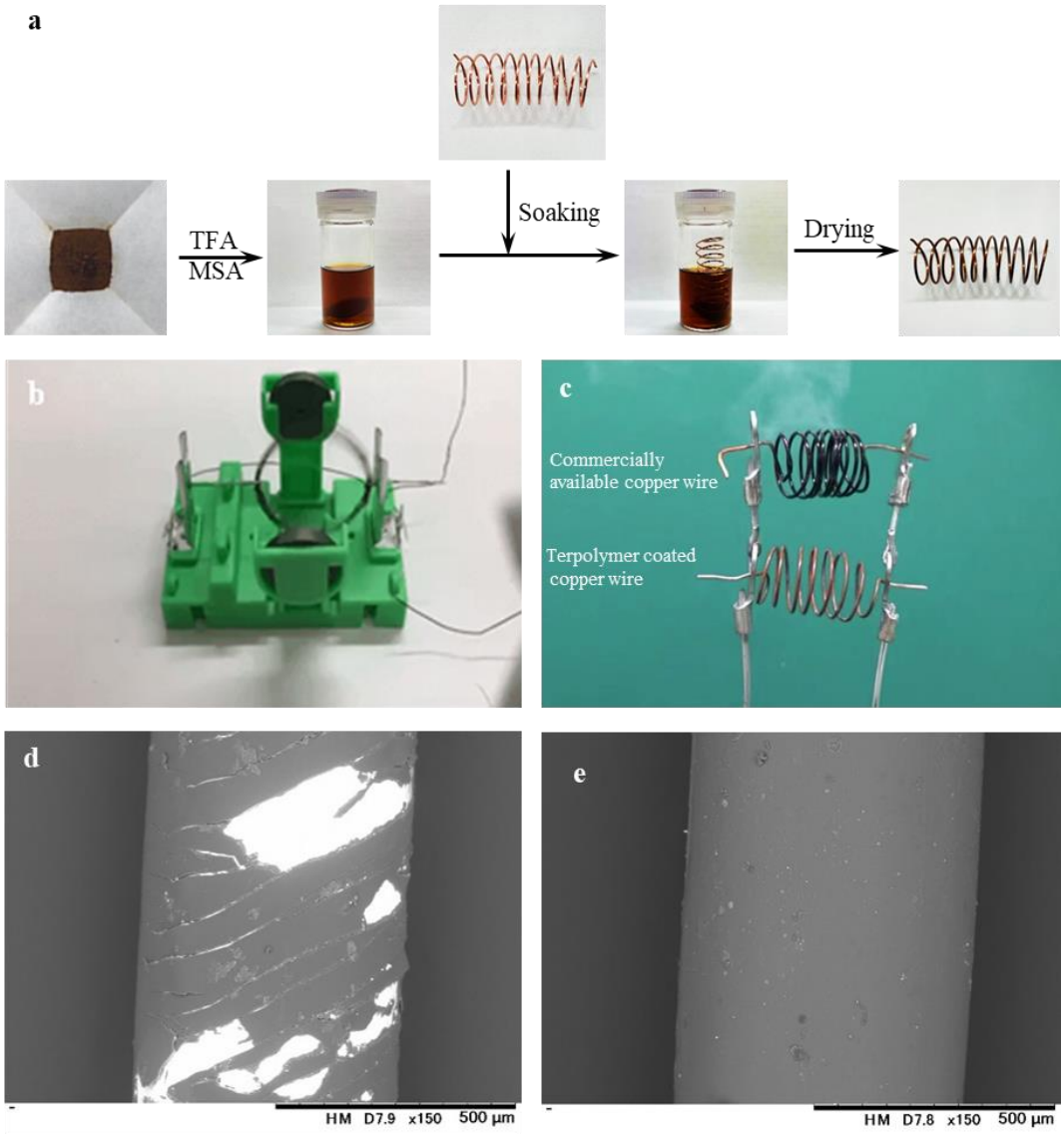

Figure 4.9. a Process of coating copper wire with terpolymer P(BI-b-BO-A). **b** Running experiment of motor, where the coil was assembled by a P(BI-b-BO-A) coated copper wire. **c** Voltage applied across the copper wires in direct current mode (upper: commercially available copper wire, lower: terpolymer coated copper wire). **d** SEM image of commercially available copper wire after applying voltage. **e** SEM image of terpolymer coated copper wire after applying voltage.

4.4 Conclusions

A series of bio-based terpolymers P(BI-*b*-BO-A) having different molar compositions of PBI, PBO and PA were successfully synthesized through a stepwise polymerization procedure, which involved the pre-polymerization of DABA followed by an additional terpolymerization with AHBA and PABA; as the simple polymerization method using all three monomers together was unsuccessful. The terpolymers thus prepared exhibited outstanding thermal, mechanical, and dielectric properties. For 30 mol% of PA, the T_{d10} reached ~760 °C, which is the highest reported for any petroleum- or bio-based plastic developed so far, and is comparable to the melting temperature of light metals. DFT calculations of the hydrogen bonding enthalpy between imidazole rings revealed how the inter-chain interactions within the polymer were strengthened by incorporating PA, which could be the reason for such ultrahigh thermoresistance of the prepared terpolymers. The highest tensile strength and strain at break for the terpolymers were found to reach up to 80 MPa and 12%, respectively, which were regulated by the molar composition of the individual monomers. The strain at break increased regularly with increase in mol% of PA. The lowest dielectric constant was found to be 2.4, which is much lower than that of most commercially available thermoresistant insulators, and comparable to that of inorganic materials such as silica. Among all the compositions,

the terpolymer in composition of 70-15-15 (mol%) exhibited a T_{d10} of 710 °C and a dielectric constant of 2.6, the appropriate amount of oxazole groups of PBO decreased the polarizability and the H-bond brought by PA increased the thermal stability, thus synergistically balanced the thermal stability and low-*k* performance and was considered to the most extraordinary one in all the compositions. Therefore, P(BI-*b*-BO-A) can be useful as an excellent insulating material for coating purposes, as was also confirmed from our coating experiment. Overall, we can conclude from all our results that the bio-based P(BI-*b*-BO-A) terpolymers have great potential to be utilized as coating materials for high power coil of high-speed electric vehicles, in the future.

4.5 References:

(1) Sadasivuni, K. K.; Saha, P.; Adhikari, J.; Deshmukh, K.; Ahamed, M. B.; Cabibihan, J. Recent Advances in Mechanical Properties of Biopolymer Composites: A Review. *Polym. Compos.* **2020**, *41* (1), 32–59.

(2) Zhao, X.-Y.; Liu, H.-J. Review of Polymer Materials with Low Dielectric Constant. *Polym. Int.* **2010**, *59* (5), 597–606.

(3) Vieira, M. G. A.; Da Silva, M. A.; Dos Santos, L. O.; Beppu, M. M. Natural-Based Plasticizers and Biopolymer Films: A Review. *European Polymer Journal*. March 2011, pp 254–263.

(4) Rajesh Banu, J.; Kavitha, S.; Yukesh Kannah, R.; Poornima Devi, T.; Gunasekaran, M.; Kim, S.-H.; Kumar, G. A Review on Biopolymer Production via Lignin Valorization. *Bioresour. Technol.* **2019**, *290*, 121790.

(5) Park, S.; Jeon, H.; Kim, H.; Shin, S.; Choy, S.; Hwang, D. S.; Koo, J. M.; Jegal, J.; Hwang, S. Y.; Park, J.; Oh, D. X. Sustainable and Recyclable Super Engineering Thermoplastic from Biorenewable Monomer. *Nat. Commun.* **2019**, *10* (1), 2601.

(6) Valerio, O.; Misra, M.; Mohanty, A. K. Sustainable Biobased Blends of Poly(Lactic Acid) (PLA) and Poly(Glycerol Succinate-Co-Maleate) (PGSMA)

with Balanced Performance Prepared by Dynamic Vulcanization. *RSC Adv.* **2017**, *7* (61), 38594–38603.

(7) Dawin, T. P.; Ahmadi, Z.; Taromi, F. A. Bio-Based Solution-Cast Blend Films Based on Polylactic Acid and Polyhydroxybutyrate: Influence of Pyromellitic Dianhydride as Chain Extender on the Morphology, Dispersibility, and Crystallinity. *Prog. Org. Coatings* **2018**, *119*, 23–30.

(8) Li, Q.; Yao, F.-Z.; Liu, Y.; Zhang, G.; Wang, H.; Wang, Q. High-Temperature Dielectric Materials for Electrical Energy Storage. *Annu. Rev. Mater. Res.* **2018**, *48* (1), 219–243.

(9) Nag, A.; Ali, M. A.; Watanabe, M.; Singh, M.; Amornwachirabodee, K.; Kato, S.; Mitsumata, T.; Takada, K.; Kaneko, T. High-Performance Poly(Benzoxazole/Benzimidazole) Bio-Based Plastics with Ultra-Low Dielectric Constant from 3-Amino-4-Hydroxybenzoic Acid. *Polym. Degrad. Stab.* **2019**, *162*, 29–35.

(10) Gordon, K. L.; Kang, J. H.; Park, C.; Lillehei, P. T.; Harrison, J. S. A Novel Negative Dielectric Constant Material Based on Phosphoric Acid Doped Poly(Benzimidazole). *J. Appl. Polym. Sci.* **2012**, *125* (4), 2977–2985.

(11) Liu, Z.-J.; Yin, C.-G.; Cecen, V.; Fan, J.-C.; Shi, P.-H.; Xu, Q.-J.; Min, Y.-L.

Polybenzimidazole Thermal Management Composites Containing Functionalized Boron Nitride Nanosheets and 2D Transition Metal Carbide MXenes. *Polymer (Guildf).* **2019**, *179*, 121613.

(12) Li, D.; Shi, D.; Xia, Y.; Qiao, L.; Li, X.; Zhang, H. Superior Thermally Stable and Nonflammable Porous Polybenzimidazole Membrane with High Wettability for High-Power Lithium-Ion Batteries. *ACS Appl. Mater. Interfaces* **2017**, *9* (10), 8742–8750.

(13) Nag, A.; Ali, M. A.; Kawaguchi, H.; Saito, S.; Kawasaki, Y.; Miyazaki, S.; Kawamoto, H.; Adi, D. T. N.; Yoshihara, K.; Masuo, S.; Katsuyama, Y.; Kondo, A.; Ogino, C.; Takaya, N.; Kaneko, T.; Ohnishi, Y. Ultrahigh Thermoresistant Lightweight Bioplastics Developed from Fermentation Products of Cellulosic Feedstock. *Adv. Sustain. Syst.* **2020**, *2000193*, 1–10.

(14) Moon, J. D.; Bridge, A. T.; D'Ambra, C.; Freeman, B. D.; Paul, D. R. Gas Separation Properties of Polybenzimidazole/Thermally-Rearranged Polymer Blends. *J. Memb. Sci.* **2019**, *582*, 182–193.

(15) Chuang, S. W.; Hsu, S. L. C.; Liu, Y. H. Synthesis and Properties of Fluorine-Containing Polybenzimidazole/Silica Nanocomposite Membranes for Proton Exchange Membrane Fuel Cells. *J. Memb. Sci.* **2007**, *305* (1–2), 353–363.

(16) Yao, F.; Xie, W.; Yang, M.; Zhang, H.; Gu, H.; Du, A.; Naik, N.; Young, D. P.; Lin, J.; Guo, Z. Interfacial Polymerized Copolymers of Aniline and Phenylenediamine with Tunable Magnetoresistance and Negative Permittivity. *Mater. Today Phys.* **2021**, *21*.

(17) Nag, A.; Ali, M. A.; Singh, A.; Vedarajan, R.; Matsumi, N.; Kaneko, T. N - Boronated Polybenzimidazole for Composite Electrolyte Design of Highly Ion Conducting Pseudo Solid-State Ion Gel Electrolytes with a High Li-Transference Number. *J. Mater. Chem. A* **2019**, *7* (9), 4459–4468.

(18) Arbuzov, A. A.; Muradyan, V. E.; Tarasov, B. P.; Sokolov, E. A.; Babenko, S. D. Epoxide Composites with Thermally Reduced Graphite Oxide and Their Properties. *Russ. J. Phys. Chem. A* **2016**, *90* (5).

(19) Yanai, T.; Tew, D. P.; Handy, N. C. A New Hybrid Exchange-Correlation Functional Using the Coulomb-Attenuating Method (CAM-B3LYP). *Chem. Phys. Lett.* **2004**, *393* (1–3)

(20) Woon, D. E.; Dunning, T. H. Gaussian Basis Sets for Use in Correlated Molecular Calculations. III. The Atoms Aluminum through Argon. *J. Chem. Phys.* **1993**, *98* (2)

(21) Simon, S.; Duran, M.; Dannenberg, J. J. How Does Basis Set Superposition Error

Change the Potential Surfaces for Hydrogen-Bonded Dimers? *J. Chem. Phys.* **1996**, *105* (24).

(22) Xu, X.; Fu, Q.; Gu, H.; Guo, Y.; Zhou, H.; Zhang, J.; Pan, D.; Wu, S.; Dong, M.; Guo, Z. Polyaniline Crystalline Nanostructures Dependent Negative Permittivity Metamaterials. *Polymer (Guildf).* **2020**, *188*.

(23) Wang, P.; Yang, L.; Gao, S.; Chen, X.; Cao, T.; Wang, C.; Liu, H.; Hu, X.; Wu, X.; Feng, S. Enhanced Dielectric Properties of High Glass Transition Temperature PDCPD/CNT Composites by Frontal Ring-Opening Metathesis Polymerization. *Adv. Compos. Hybrid Mater.* **2021**, *4* (3).

(24) Strella, S.; Zand, R. Dielectric Studies of the Methacrylate Series. II. Poly-n-Butyl Methacrylate. *J. Polym. Sci.* **1957**, *25* (108), 105–114.

(25) Czech, Z.; Agnieszka, K.; Ragańska, P.; Antosik, A. Thermal Stability and Degradation of Selected Poly(Alkyl Methacrylates) Used in the Polymer Industry. *J. Therm. Anal. Calorim.* **2015**, *119* (2), 1157–1161.

(26) Yu, S.; Hing, P.; Hu, X. Dielectric Properties of Polystyrene–Aluminum-Nitride Composites. *J. Appl. Phys.* **2000**, *88* (1), 398–404.

(27) ARII, T. TG-MS Study on Thermal Decomposition of Polystyrene. *J. Mass Spectrom. Soc. Jpn.* **2003**, *51* (1), 235–241.

(28) Yuan, X.; Matsuyama, Y.; Chung, T. C. M. Synthesis of Functionalized Isotactic Polypropylene Dielectrics for Electric Energy Storage Applications. *Macromolecules* **2010**, *43* (9), 4011–4015.

(29) Esmizadeh, E.; Tzoganakis, C.; Mekonnen, T. H. Degradation Behavior of Polypropylene during Reprocessing and Its Biocomposites: Thermal and Oxidative Degradation Kinetics. *Polymers (Basel).* **2020**, *12* (8), 1627.

(30) Simpson, J. .; St.Clair, A. . Fundamental Insight on Developing Low Dielectric Constant Polyimides. *Thin Solid Films* **1997**, *308–309* (1–4), 480–485.

(31) Huo, P.; Cebe, P. Dielectric Relaxation of Poly(Phenylene Sulfide) Containing a Fraction of Rigid Amorphous Phase. *J. Polym. Sci. Part B Polym. Phys.* **1992**, *30* (3), 239–250.

(32) Sun, H.; Lv, Y.; Zhang, C.; Zuo, X.; Li, M.; Yue, X.; Jiang, Z. Materials with Low Dielectric Constant and Loss and Good Thermal Properties Prepared by Introducing Perfluorononenyl Pendant Groups onto Poly(Ether Ether Ketone). *RSC Adv.* **2018**, *8* (14)

(33) Patel, P.; Hull, T. R.; McCabe, R. W.; Flath, D.; Grasmeder, J.; Percy, M. Mechanism of Thermal Decomposition of Poly(Ether Ether Ketone) (PEEK) from a Review of Decomposition Studies. *Polym. Degrad. Stab.* **2010**, *95* (5),

709–718.

(34) Tanthapanichakoon, W.; Furuuchi, M.; Nitta, K.; Hata, M.; Endoh, S.; Otani, Y. Degradation of Semi-Crystalline PPS Bag-Filter Materials by NO and O2 at High Temperature. *Polym. Degrad. Stab.* **2006**, *91* (8), 1637–1644.

(35) Lua, A. C.; Su, J. Isothermal and Non-Isothermal Pyrolysis Kinetics of Kapton® Polyimide. *Polym. Degrad. Stab.* **2006**, *91* (1), 144–153.

(36) Gu, H.; Xu, X.; Cai, J.; Wei, S.; Wei, H.; Liu, H.; Young, D. P.; Shao, Q.; Wu, S.; Ding, T.; Guo, Z. Controllable Organic Magnetoresistance in Polyaniline Coated Poly(p -Phenylene-2,6-Benzobisoxazole) Short Fibers. *Chem. Commun.* **2019**, *55* (68), 10068–10071.

(37) Kuroki, T.; Tanaka, Y.; Hokudoh, T.; Yabuki, K. Heat Resistance Properties of Poly(p-Phenylene-2,6-Benzobisoxazole) Fiber. *J. Appl. Polym. Sci.* **1997**, *65* (5), 1031–1036.

Chapter V

General conclusion

Chapter V

5.1 General conclusions

Polybenzazoles series of polymers are successfully synthesized from bio-derived resources and the properties of them are characterized. The distinct structure endowed these polymers extremely high thermoresitance and relatively outstanding dielectric performance.

In chapter 2, PBO-co-PBI series of copolymers present different variation in thermal stability from the homopolymers. 2,6-PBO-co-PBI exhibit higher thermal stability than another copolymer. The films were successfully fabricated by the copolymer 2,6-PBO-co-PBI, and the higher molar composition of PBI tends to present more durable film.

In chapter 3, Monomer AMBA and copolymer PBT-co-PBI were successfully synthesized, the mechanical, thermal and dielectric properties of the copolymers was characterized. The obtained film showed an ultrahigh thermal stability, thermal decomposition temperatures decrease when increase the ratios of PBT, the highest 10% weight loss temperature reaches 760 degrees, higher than most organic materials, even comparable with some inorganic materials. Copolymer films in all compositions present high dielectric performance with dielectric constant around 3 and volume resistivity higher than $10^{14}\,\Omega\cdot\mathrm{cm}$ in dry state. The elongation of films can be optimized via doping

experiment. The elongation at break of film in 20/80 mol% composition reaches 150%, indicating the copolymer can be used as high performance thermostable insulating films.

In chapter 4, terpolymer with a block structure was synthesized through a stepwise polymerization procedure, which involved the pre-polymerization of DABA followed by an additional terpolymerization with AHBA and PABA; as the simple polymerization method using all three monomers together was unsuccessful. The terpolymers thus prepared exhibited outstanding thermal, mechanical, and dielectric properties. For 30 mol% of PA, the T_{d10} reached ~760 °C, which is the highest reported for any petroleum- or bio-based plastic developed so far, and is comparable to the melting temperature of light metals. DFT calculations of the hydrogen bonding enthalpy between imidazole rings revealed how the inter-chain interactions within the polymer were strengthened by incorporating PA, which could be the reason for such ultrahigh thermoresistance of the prepared terpolymers. The highest tensile strength and strain at break for the terpolymers were found to reach up to 80 MPa and 12%, respectively, which were regulated by the molar composition of the individual monomers. The strain at break increased regularly with increase in mol% of PA. The lowest dielectric constant was found to be 2.4, which is much lower than that of most commercially available thermoresistant insulators, and comparable to that of inorganic materials such as silica.

Therefore, P(BI-*b*-BO-A) can be useful as an excellent insulating material for coating purposes, as was also confirmed from our coating experiment. Overall, we can conclude from all our results that the bio-based P(BI-*b*-BO-A) terpolymers have great potential to be utilized as coating materials for high power coil of high-speed electric vehicles, in the future.

Research achievements

Papers:

Submitted:

1. Design of biopolybenzazole exhibiting low dielectric constant and ultrahigh thermoresistance, **Xianzhu Zhong**, Aniruddha Nag, Jiabei Zhou, Kenji Takada, Fitri Adila Amat Yusof, Tetsu Mitsumata, Kenji Oqmhula , Kenta Hongo, Ryo Maezono,Tatsuo Kaneko

Under preparation:

1. Syntheses and characterizations of poly{benzothiazole-co-benzimidazole} showing high thermal stability, **Xianzhu Zhong**, Mohannad Asif Ali, Aniruddha Nag, Jiabei Zhou, Kenji Takada, Tatsuo Kaneko
2. Deuterium replacement of polybenzimidazole-amide copolymer and preparation of ultrahigh heat resistant film, **Xianzhu Zhong,** Motoyuki Kusano, Aniruddha Nag, Kenji Takada, Tatsuo Kaneko
3. Preparation of bio-based polybenzimidazole-co-polyamide showing high toughness, **Xianzhu Zhong,** Nakajima Akinori, Aniruddha Nag, Kenji Takada, Tatsuo Kaneko

Conferences:

Domestic Conference:

1. Poster title: Syntheses of bio-Based and wholly-Aromatic benzazoles with ultra-high-thermoresistance, **Xianzhu Zhong**, Aniruddha Nag, Kenji Takada, Tatsuo Kaneko, 68th Symposium on Macromolecules, Fukui University, 25-17 September, 2019.

International Conferences:

2. Poster title: Super-thermoresistance in bio-based benzazoles from wholly-aromatic amino acids, **Xianzhu Zhong**, Aniruddha Nag, Kenji Takada, Tetsu Mitsumata, Tatsuo Kaneko, Asia Pacific Society for Materials Research 2019 Annual Meeting, Hokdaido, 26-29 July, 2019.
3. Poster title: Syntheses of bio-based and wholly-aromatic benzazoles with high thermoresistance and insulation performance, **Xianzhu Zhong**, Aniruddha Nag, Kenji Takada, Tatsuo Kaneko, 15th IUPAC International Conference on Novel Materials and their Synthesis (NMS-XV), Shenyang, 6-11 September, 2019.
4. Poster title: Development of bio-based and wholly aromatic polybenzazoles with ultrahigh thermoresistance and low-k dielectric performance, **Xianzhu Zhong**, Aniruddha Nag, Gewinner Sinaga, JAIST world conference 2020, Kenji Takada,

Tetsu Mitsumata, Tatsuo Kaneko, JAIST, 10 November, 2020.

Awards:

1. Doctoral Research Fellowship (DRF), from April 2019 to March 2022.
2. The Third Poster Prize, Asia Pacific Society for Materials Research 2019 Annual Meeting, 27 July, 2019

Research Fund:

1. JAIST Research Grants (Houga) 2020.

ACKNOWLEDGEMENT

The research presented in this dissertation was performed in Kaneko laboratory, Japan Advanced Institute of Science and Technology, during the period from April 2019 to July 2022, financially supported by Cross-ministerial Strategic Innovation Promotion Program (SIP), “Smart-bio” (Bio-oriented Technology Research Advancement Institution, NARO), Japan and JAIST Research Grants (Hoga) 2020.

I would like to express my sincere gratitude to my supervisor Prof. Tatsuo Kaneko for his valuable guidance, suggestions and continuous support during the whole research. He is such an amiable professor of broad knowledge that I feel it a great pleasure to study and work under his guidance. Prof. Kaneko always shows great patience and understanding to the mistakes made in my experiments, which makes it possible for me to freely carry out the research and explore in the related fields without any hesitation. Obviously, this research is impossible to be completed without his kind encouragement and constructive guidance.

I am grateful to Prof. Tetsu Mitsumata for his permission to perform the dielectric experiment in his laboratory, he offered kind help not only during the experiment but

also in the entire dielectric research.

I am also thankful to Prof. Toshiake Taniike for his helpful suggestions as my second supervisor.

I would like to thank Prof. Noriyoshi Matsumi for his value advice and kind help in my minor and main researches.

I am also grateful to Dr. Kenji Takada, for his continuous help and suggestions in my research. His professional advice helped a lot throughout the research. Besides, he offered great convenience for experiment as well in the laboratory.

I would like to convey my grateful acknowledgement to Prof. Toshiake Taniike, Prof. Noriyoshi Matsumi, and Prof. Kazuaki Matsumura of JAIST and Prof. Tsuyohiko Fujigaya of Kyushu University for their assistance to complete this dissertation.

I would also like to express my appreciation to Dr. Maiko Okajima for her encouragement and kind help throughout the whole research. Many thanks to her kind concern about the research and life situation of the whole lab members.

My sincere appreciation to Dr. Mohammad Asif Ali and Dr. Anuruddha Nag for their useful guidance suggestions during the whole research.

I would also like to thank Mr. Jiabei Zhou for his help in experiment, and to all the members of Kaneko laboratory, thanks to them for their kind help and assistance in

research and life, especially for their efforts in creating the greatest laboratory atmosphere.

Finally, I would like to express my special thanks my families, they have always been supporting me in any problems. All my achievements can be attributed to their support and understanding.

June 2022

Xianzhu Zhong